water

MDPI

Article

Phytoplankton Diversity and Co-Dependency in a Stratified Oligotrophic Ecosystem in the South Adriatic Sea

Antonija Matek [1], Maja Mucko [1], Raffaella Casotti [2], Anna Chiara Trano [2], Eric P. Achterberg [3], Hrvoje Mihanović [4], Hrvoje Čižmek [5], Barbara Čolić [5], Vlado Cuculić [6] and Zrinka Ljubešić [1,*]

1 Department of Biology, Faculty of Science, University of Zagreb, 10000 Zagreb, Croatia; antonija.matek@biol.pmf.hr (A.M.); maja.mucko@biol.pmf.hr (M.M.)
2 Department of Integrative Marine Ecology, Stazione Zoologica Anton Dohrn, Villa Comunale, 80121 Naples, Italy; raffaella.casotti@szn.it (R.C.); annachiara.trano@szn.it (A.C.T.)
3 GEOMAR Helmholtz Centre for Ocean Research Kiel, 24148 Kiel, Germany; eachterberg@geomar.de
4 Institute of Oceanography and Fisheries, 21000 Split, Croatia; hrvoje.mihanovic@izor.hr
5 Marine Explorers Society 20.000 Leagues, 23000 Zadar, Croatia; hrvoje@drustvo20000milja.hr (H.Č.); bcolic@drustvo20000milja.hr (B.Č.)
6 Division for Marine and Environmental Research, Ruđer Bošković Institute, 10000 Zagreb, Croatia; vlado.cuculic@irb.hr
* Correspondence: zrinka.ljubesic@biol.pmf.hr

Abstract: The oligotrophy of the southern Adriatic Sea is characterized by seasonal stratification which enables nutrient supply to the euphotic layer. A set of interdisciplinary methods was used to elucidate the diversity and co-dependency of bacterio- and phytoplankton of the water column during the stratification period of July 2021. A total of 95 taxa were determined by microscopy: 58 diatoms, 27 dinoflagellates, 6 coccolithophores, and 4 other autotrophs, which included Chlorophyceae, Chrysophyceae, and Cryptophytes. Nanophytoplankton abundances were higher in comparison to microphytoplankton. The prokaryotic plankton community as revealed by HTS was dominated by Proteobacteria (41–73%), Bacteroidota (9.5–27%), and cyanobacteria (1–10%), while the eukaryotic plankton community was composed of parasitic Syndiniales (45–80%), Ochrophyta (2–18%), Ciliophora (2–21%), Chlorophytes (2–4%), Haptophytes (1–4%), Bacillariophyta (1–13%), Pelagophyta (0.5–12%) and Chrysophyta (0.5–3%). Flow cytometry analysis has recorded *Prochlorococcus* and photosynthetic picoeukaryotes as more abundant in deep chlorophyll maximum (DCM), and *Synechococcus* and heterotrophic bacteria as most abundant in surface and thermocline layers. Surface, thermocline, and DCM layers were distinct considering community diversity, temperature, and nutrient correlations, while extreme nutrient values at the beginning of the investigating period indicated a possible nutrient flux. Nutrient and temperature were recognized as the main environmental drivers of phytoplankton and bacterioplankton community abundance.

Keywords: phytoplankton; bacterioplankton; diversity; co-dependency; stratification; oligotrophic ecosystem; South Adriatic Sea; Mediterranean

Citation: Matek, A.; Mucko, M.; Casotti, R.; Trano, A.C.; Achterberg, E.P.; Mihanović, H.; Čižmek, H.; Čolić, B.; Cuculić, V.; Ljubešić, Z. Phytoplankton Diversity and Co-Dependency in a Stratified Oligotrophic Ecosystem in the South Adriatic Sea. *Water* **2023**, *15*, 2299. https://doi.org/10.3390/w15122299

Academic Editor: Jun Yang

Received: 21 March 2023
Revised: 12 June 2023
Accepted: 15 June 2023
Published: 20 June 2023

1. Introduction

Distribution patterns of primary producers are determined by a combination of physico-chemical (e.g., light availability, nutrient supply, water column stratification) and biological processes (e.g., microbial activity, grazing, viral lysis) [1]. Due to ongoing climate change, which is progressively warming the ocean, we are witnessing more stratified water columns with a decrease in mixing and subsurface nutrient supply to the euphotic layer. It is important to understand the mechanisms of nutrient supply and to identify potential hot spot regions of enhanced net primary production, for example, along shelf breaks, in upwelling regions and areas of enhanced dynamic mixing.

The climatically temperate Adriatic Sea experiences a bimodal seasonal variability in phytoplankton biomass, typically with maxima in spring and autumn [2,3]. While picophytoplankton dominates the phytoplankton community in the southern Adriatic Sea and appears to be the overall dominant primary producer [4,5], microphytoplankton production is restricted to coastal waters, the deep chlorophyll maximum (DCM), and periods during or following winter convection [6–9]. Winters in the southern Adriatic Sea are characterized by convection events and vertical mixing that occur regularly, supporting nutrient supply to surface waters that facilitates phytoplankton development [6,7,9]. Ultimately, these larger scale physical processes impact the whole food web of exceptionally high summer anchovy catches following a higher than usual abundance of phytoplankton in the winter of 2015 [10].

Upwelling on the Palagruža Sill was detected by enhanced nutrient concentrations and abundance of primary producers [10]. Similarly, a small peak in nutrient concentrations and nano- and picophytoplankton abundance was recorded close to the Lastovo Island cliffs, indicating a possible upwelling effect near the island [5,10]. However, satellite images do not show enhanced primary production under stratified conditions (Mihanović, personal communication). A possible explanation may be a rapid uptake of nutrients with efficient, almost instant, removal of primary producers by zooplankton under oligotrophic conditions [11]. In a flexible biome, such as the one of the Adriatic Sea, the first signals of climate-driven changes might be represented by the spatial reorganization of communities [12]. These findings suggest that climate change might be impacting the biological structure of this basin more rapidly as compared to the large oceans, suggesting the Adriatic Sea as an ideal environment model for plankton diversity and co-dependency investigations.

Recently, an interesting oceanographic phenomenon, known as island-trapped waves (ITW), has been recognized around Lastovo Island in the Adriatic Sea [13,14], making it together with Bermuda [15,16], Hawaii [17,18], Gotland in the Baltic Sea [19], and Saint Pierre and Miquelon archipelago in the northwestern Atlantic Ocean [20], one of the only islands in the world where such waves were observed. The link between those physical processes and ecosystem diversity and functioning has not yet been fully explored and described. The significance of this study is to explain phytoplankton/bacterioplankton diversity and co-dependency in the ecosystem of Lastovo Island to have a basis for comparison of the ecosystem response to observed island effects. Therefore, the aims of the study are as follows: (1) to investigate phytoplankton and bacterioplankton diversity in an oligotrophic ecosystem of the Adriatic Sea during a period of water column stratification, and (2) to analyse the co-dependency of phytoplankton and bacterioplankton communities.

2. Materials and Methods

2.1. Study Area

The Adriatic Sea is a semi-enclosed oligotrophic basin approximately 800 km long and 200 km wide and is elongated in a northwest–southeast direction. It is of interest due to its numerous large and small islands and islets along the eastern coast. Lastovo Island, located in the southern part of the middle Adriatic Sea island group, is characterized by very steep island sides and has average depths reaching 70 m at about 300 m from the island (Figure 1).

Physical processes relevant for the island of Lastovo include resonantly excited diurnal internal waves that revolve around the island in a clockwise direction (island-trapped waves). These waves result in diurnal thermocline oscillations ranging up to 30 m during stratification periods [21]. The lower diversity of bryozoans and other benthic organisms between the surface and 40 m depth at Lastovo's submersed cliffs compared with other Adriatic locations is thought to be due to large diurnal and intertidal temperature fluctuations during the summer stratification periods [21,22]. Additionally, in the area around Lastovo Island, relatively high chlorophyll *a* (Chl *a*) concentrations were recorded [10,23], which contrasts with other parts of the oligotrophic southern Adriatic Sea [4,8,23,24].

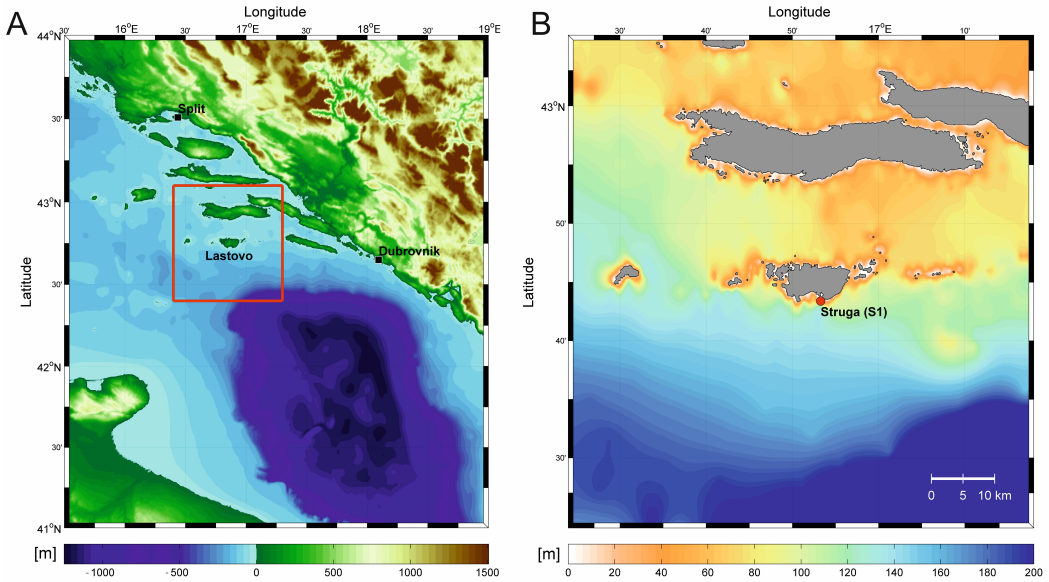

Figure 1. Location of study area (Lastovo Island, South Adriatic Sea) (**A**) and sampling station Struga (S1) (**B**) superimposed on bathymetry maps.

2.2. Sampling

During the stratification period in 2021, a set of thermistors was deployed at nine equidistant depths between 5 and 45 m at the rocky cliffs of Lastovo Island (Figure 1). Six loggers were recovered at the end of measurement period, as loggers positioned at 15, 25, and 40 m were either missing or not functioning properly. The measurement interval was 5 min. A ship-based survey was conducted in the period from 12 to 21 July 2021. T–S–Chl F (temperature, salinity, Chl *a* fluorescence) profiles were measured using an SBE 25 CTD probe (Sea-Bird Electronics Inc., Bellevue, WA, USA) twice a day, at around 06:00 (UTC+2), when a deep thermocline was expected at the location, and at around 18:00 (UTC+2), when a shallow thermocline was expected. Complementary to the CTD casts, water samples for flow cytometry, nutrient, Chl *a*, and phytoplankton analyses were collected using 5 L Niskin bottles at one station at depths determined in situ based on the position of the thermocline (Supplementary Table S1). Samples for flow cytometry measurements of picoplankton abundance were taken in duplicate, where 1.5 mL of sample was fixed with 100 µL of glutaraldehyde (36%), deep frozen in liquid nitrogen, and stored at −80 °C until analysis.

Triplicates of 15 mL sample were taken for nutrient analysis, filtered through a 0.2 µm syringe filter, fixed with 30 µL of 6 M HCl, and stored in the dark and cold until the analysis in the laboratory. Samples of 1 L volume for Chl *a* analysis were filtered in situ using 0.7 µm pore size Whatman GF/Fs (Cytiva Whatman glass microfiber filters, Marlborough, MA, USA) and preserved in –80 °C liquid nitrogen until the analysis.

Discrete and net phytoplankton samples were fixed with 2% neutralized formaldehyde and stored in 250 mL bottles until analysis in the laboratory. Water samples for environmental DNA (eDNA) extraction and small ribosomal units of bacteria and eukaryote (16S rRNA and 18S rRNA genes) analysis were taken with Niskin bottles from surface (0 m) and DCM (75 m) waters. A total of nine samples were taken: six samples on 13 of July 2021 and three samples on 20 of July 2021 (Supplementary Table S2). A large volume (approx. 6 L) of seawater was filtered through 20 µm, then 3 µm, and ultimately 0.2 µm pore-size polycarbonate filters (Cytiva Whatman Cyclopore, Marlborough, MA, USA) to obtain plankton size-fractions: pico-nanoplankton (0.2–3 µm), nanoplankton (3–20 µm), and micro-mesoplankton (>20 µm). Filters were immediately frozen in liquid nitrogen and transferred to the laboratory where they were stored at −80 °C until eDNA extraction.

2.3. Plankton Community and Nutrient Analysis

Light microscopy (LM) was used to determine microphytoplankton (>20 µm) and nanophytoplankton (2–20 µm) composition and abundance. Subsamples of 100 mL were settled for 48 h and analyzed under a Zeiss Axiovert 200 inverted microscope (Carl Zeiss microscopy GmbH, Jena, Germany) using the Utermöhl method [25]

Abundances of heterotrophic bacteria and cyanobacteria were determined on a BD FACSVerse flow cytometer (BD Biosciences, Franklin Lake, NJ, USA) equipped with a standard filter setup and with 488 nm laser excitation, as described in Babić et al., 2018 [26].

Phosphate (PO_4), nitrate (NO_3), nitrite (NO_2), and silicic acid (SiO_4) concentrations were analysed using an autoanalyzer (SEAL QuAAtro segmented flow AutoAnalyzer, SEAL Analytical GmbH, Norderstedt, Germany), with procedures as per international GO-SHIP protocols [27]. KANSO-certified reference materials were used to verify the accuracy of the analysis. Chl *a* was analysed by the fluorometric procedure after extraction in 90% acetone [28]. The detection limit for Chl *a*, considering the filtered volume of water, was 0.01 μgL^{-1}.

2.4. eDNA Isolation, Amplicon Sequencing and Bioinformatics

eDNA was extracted from polycarbonate filters by using a DNeasy PowerSoil kit (Qiagen, Hilden, Germany), following the manufacturer's instructions with minor changes. Modifications involved mechanical disruption by vortex on a VortexGenie 2 (Fisher Scientific, Waltham, MA, USA) for 15 min at maximum speed and incubation at 37 °C for 30 min with the addition of 2 µL of lysozyme (0.5 mg mL^{-1} solution). Extracted DNA yield and quality were measured by Qubit fluorometer (Thermo Fisher, Waltham, MA, USA), while the integrity of DNA was checked on 1% agarose gel. Samples of total extracted DNA were sent for 16S rRNA and 18S rRNA gene library preparation and amplicon next-generation sequencing to the FISABIO–Public Health Sequencing and Bioinformatics Service (Servicio de Secuenciación y Bioinformática, Valencia, Spain). Sequencing was performed on the Illumina MiSeq (Illumina, Chesterfield, UK) platform following the manufacturer's guidelines. The 16S rRNA gene V4–V5 variable region was targeted by PCR primers from Earth Microbiome Project 515F and 806R primers: (FWD: 5′-GTGYCAGCMGCCGCGGTAA-3′; REV: 5′-GGACTACNVGGGTWTCTAAT-3′), while the 18S rRNA gene V4 variable region was targeted by PCR primers Reuk454FWD1 (5′-CCAGCASCYGCGGTAATTCC-3′) and ReukREV3 modified (5′-ACTTTCGTTCTTGATYRATGA-3′), with a barcode on the forward primer. The PCR program included a 28-cycle PCR using the HotStarTaq Plus Master Mix Kit (Qiagen, Germantown, MD, USA) under the following conditions: 94 °C for 3 min, followed by 28 cycles of 94 °C for 30 s, 53 °C for 40 s, and 72 °C for 1 min, with a final elongation step at 72 °C for 5 min. PCR products were visualized on 2% agarose gel to check the success of amplification and the relative intensity of bands.

Quality of raw reads was checked with FastQC ver.0.11.5. [29], after which reads were processed using QIIME 2 2021.11 [30] in a pipeline composed of several steps: importing and demultiplexing of raw sequence data, quality filtering and denoising using DADA2 plugin [31], and taxonomy assignment of the resulting amplicon sequencing variants (ASVs) using a Naïve Bayes classifier pre-trained on the latest version SILVA database for prokaryotes and the PR2 database for eukaryotes with a 99% OTU identity threshold [32]. For the 16S rRNA dataset, from a total of 1,735,345 raw reads, 1,453,307 were included in further analysis, while for the 18S rRNA dataset, from a total of 1,262,960 raw reads, 858,740 were included for further analysis. To subsample the datasets, taxa filtering was performed to exclude chloroplast, mitochondrial, and archaeal sequences from the 16S rRNA dataset and chloroplast, mitochondrial, and metazoan sequences from 18S rRNA dataset, focusing only on bacteria and cyanobacteria in the 16S dataset and true contributors to pico-, nano-, and microplankton in the 18S dataset. Further taxa filtering for 18S dataset was conducted to include only classes of taxa revealed by light microscopy (Dinophyta, Bacillariophyta, Chlorophyta, Haptophyta, and Cryptophyta), thus, showing comparable results and allowing us to compare morphological identification with 18S rRNA gene

affiliation. Raw sequences are deposited in the European Nucleotide Archive (ENA) under project number PRJEB59876.

The cladogram (tree containing representative sequences from filtered dataset) was constructed using plugin q2-phylogeny: the MAFFT program was used to perform multiple sequence alignment, masking ambiguously aligned regions and applying FastTree for creating a cladogram from the masked alignment. The generated tree had 1070 sequences and was visualized in iTOL 4.4.2. [33]. The taxonomy dataset generated in QIIME2 using PR2 database [Taxonomy.qza] was added to the visualization of the tree to apply leaf identification. Sequences that were poorly identified or defined as "uncultured" were searched in the NCBI GenBank database using the BLAST search tool, and those with a low identity threshold were pruned from the tree. We additionally pruned out identical sequences that taxonomically corresponded to the same species or strain. The final tree was composed of 211 relevant taxa spread through Dinophyta, Cryptophyta, Haptophyta, Chlorophyta, and Bacillariophyta. The sample frequency (number of ASVs identified as an individual representative sequence) was added using FeatureTable [Frequency] (Supplementary Figure S1). Taxa bar plots visualization were performed in RStudio version 1.2.1335, using the 'qiime2R' [34], 'phyloseq' [35], and 'ggplot2' [36] packages.

2.5. Statistical Analyses

For the purposes of data visualization and statistical analyses, sampling depths were grouped into three categories: surface, thermocline, and deep chlorophyll *a* maxima layer (DCM) according to temperature (surface and thermocline) and Chl *a* concentration (DCM) (Supplementary Table S1). The values were as follows: surface layer, 22.6–25.5 °C; thermocline layer, 17.3–22.3 °C; DCM layer, 0.120–0.222 μgL^{-1}.

Statistical analyses were performed in Primer 7.0. (Primer-E Ltd. 2021, Auckland, New Zealand) and in R studio using 'vegan' [37] and 'Hmisc' [38] packages. Data editing and reading in R studio were performed using the 'tidyverse' [39], 'tibble' [40], and 'readr' [41] packages. Prior to statistical analyses, plankton community data including phytoplankton and bacterioplankton counts were log-transformed, while environmental data were log-transformed, normalized, and standardized. Transformations were carried out in order to create resemblance matrices and to combine them in correlation analysis, canonical correspondence analyses, and principal component analysis.

Phytoplankton community diversity was defined by calculating biodiversity indices, and dominant taxa were determined by maximum abundances and frequency of appearance in samples. Significant average dissimilarity in phytoplankton community and nutrient composition between the surface, thermocline, and DCM layers were tested using analysis of similarities (ANOSIM). The contribution of dominant taxa to the observed dissimilarity of water layers was determined using similarity percentage analysis (SIMPER).

Nutrient and Chl *a* distribution in the water column and changes over the investigating period were analyzed in Primer using principal component analysis (PCA). The significance of clusters revealed by PCA was tested using ANOSIM, performed within the two factors (factor period and factor water column), determined by differences visualized with linear scatter plots. Prior to ANOSIM, a resemblance matrix was calculated using Euclidean distance for environmental data, and Manhattan distance (Bray–Curtis similarity) for biotic data.

Spearman's rank correlation analysis was carried out between the environmental data. Furthermore, a percentage of plankton community variability that can be explained by environmental variables was calculated using canonical correspondence analyses (CCAs). The model used nutrients as constrained variables for bacterioplankton and phytoplankton data. Variance inflation factors were calculated for each constraint in order to eliminate those which are highly correlated from the model, making the CCA more constrained. Statistical significance of the CCA model and constrained axes was tested using analysis of variance (ANOVA).

3. Results

3.1. Water Column Structure

Vertical profiles of temperature at station Struga elucidate a stratified water column with intermittent diurnal vertical thermocline oscillations. Chl *a* fluorescence (Chl F) retrieved by CTD cast elucidated a DCM layer that followed the thermocline oscillation, showing diurnal depth variations with maximum values observed from a 30 to 70 m depth (Figure 2).

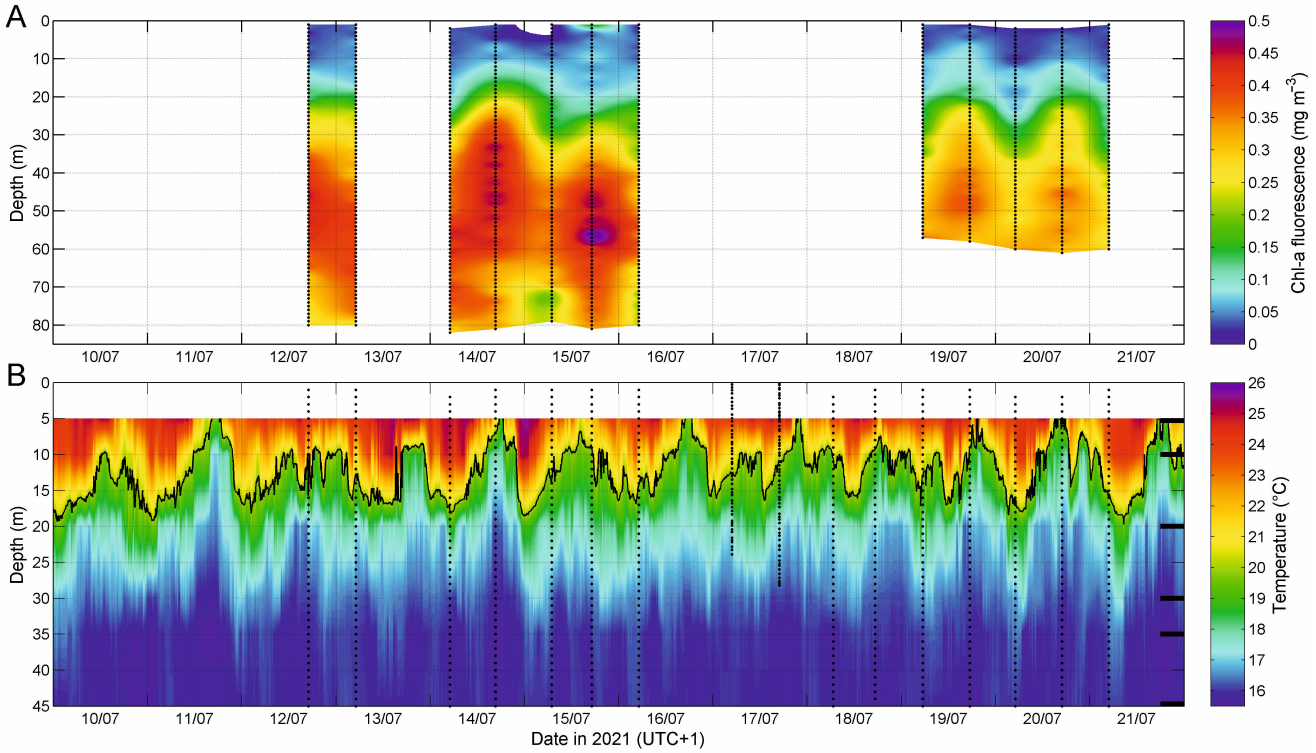

Figure 2. Chlorophyll *a* (Chl *a*) fluorescence vertical profiles recovered from CTD casts (**A**) and temperature data recorded on loggers from the cliff at S1 station (**B**). Vertical dotted lines indicate CTD casts. Black horizontal ticks in panel (**B**) indicate deployment depths of recovered temperature loggers.

Maximum Chl *a* concentration in the DCM, thermocline, and surface layers was 0.222 μgL^{-1}, 0.098 μgL^{-1}, and 0.071 μgL^{-1}, respectively. Three peaks of Chl *a* concentration in the DCM layer through investigated period were recorded on 12, 14, and 20 July (Figure 3). Maximum NO_2 concentration was 0.013 $\mu mol\ L^{-1}$ at the surface, while NO_3, PO_4, and SiO_4 reached their maximum in the DCM layer with concentrations of 10.26 $\mu mol\ L^{-1}$, 0.761 $\mu mol\ L^{-1}$, and 3.530 $\mu mol\ L^{-1}$, respectively. Nutrient concentrations were higher at the beginning of the study period, and then significantly decreased by the end (Figure S3A and Figure 3). Maximal values of NO_3, PO_4, and SiO_4 in the thermocline and DCM layer were recorded on 12 July with second peak after 14 July, while in the surface layer the maximal values of NO_3, PO_4, and SiO_4 were recorded on the 15 July 2021 (Figure 3).

In the stratified water column, nutrients exhibited significant distinct vertical distribution confirmed by PCA (Supplementary Figure S2) and the ANOSIM test (Supplementary Figure S3B). PCA elucidated a trend of increases in PO_4 and NO_2 concentrations in the surface and thermocline layers, and NO_3 and SiO_4 in DCM layer (Supplementary Figure S2). PC 1 and PC 2 axes explain 49.6% and 73.4% of the total data variability, respectively. Temperature and NO_3 had the highest correlation with the PC 2 and PC 1 axes, respectively (Supplementary Table S3).

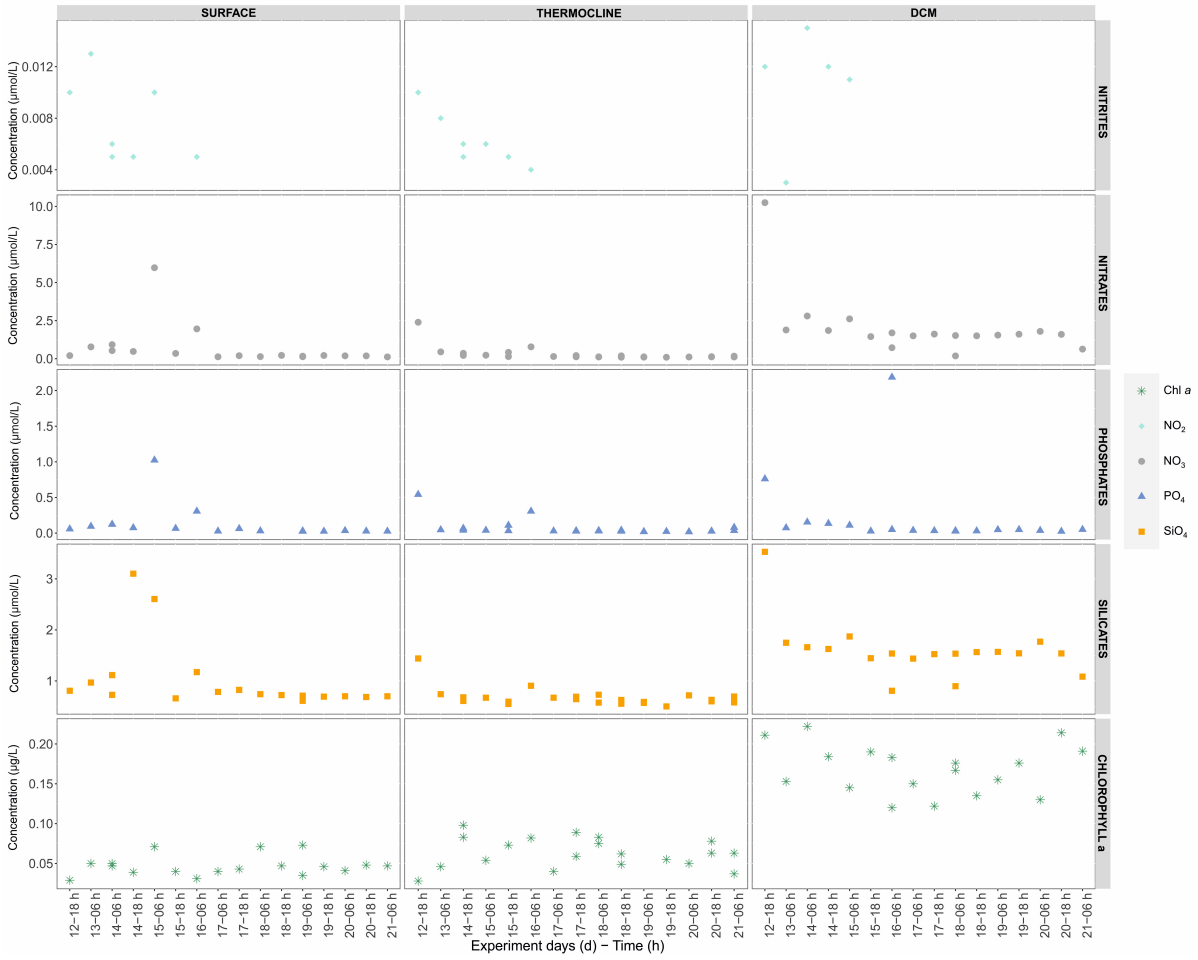

Figure 3. Chl *a*, nitrite (NO_2), nitrate (NO_3), phosphate (PO_4), and silicate (SiO_4) concentrations during the study period (12–21 July 2021).

3.2. Phytoplankton Community Diversity

3.2.1. Taxonomic Composition and Abundance

A total of 95 taxa were determined, of which there were 58 diatoms, 27 dinoflagellates, 6 coccolithophores, and 4 other autotrophs, which included chlorophyceae, chrysophyceae, and cryptophytes (Supplementary Table S4). The microphytoplankton community was dominated by diatoms (36.5%), while dinoflagellates (3.2%) and coccolithophores (0.6%) contributed less. Nanophytoplankton was comprised of dinoflagellates (37.8%), coccolithophores, (6.8%), and other autotrophs (15.1%) (Figure 4).

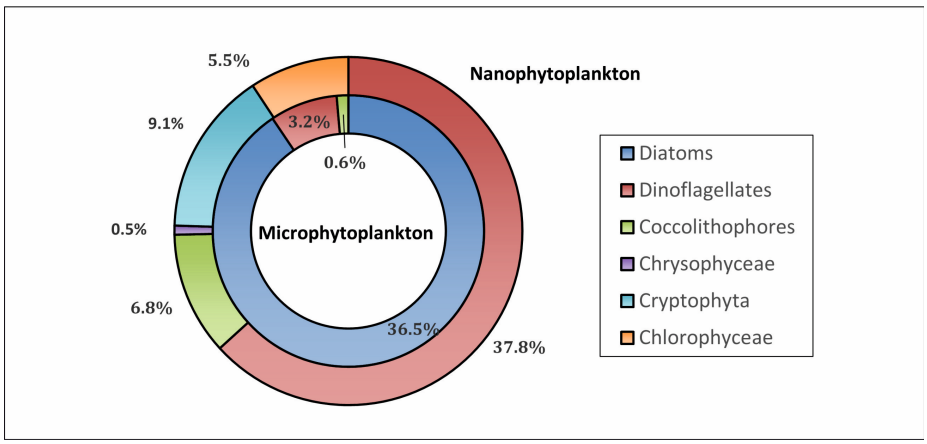

Figure 4. Phytoplankton taxonomic composition at station Struga (S1), Lastovo Island.

The maximum recorded cell abundance was 23.4 × 10^3 cells L^{-1} (Supplementary Table S4), and the species richness was 10.2 (Supplementary Table S5). Maximal nanophytoplankton and microphytoplankton abundance was 36.9 × 10^3 cells L^{-1} and 28 × 10^3 cells L^{-1}, respectively (Figure 5). The phytoplankton community had uneven species distribution, as confirmed by Pielou's evenness ($J' = 0.58$) (Supplementary Table S5). Shannon–Weiner ($H' = 2.67$), and Simpson diversity index ($1 - \lambda' = 0.84$) confirmed a low phytoplankton community diversity (Supplementary Table S5).

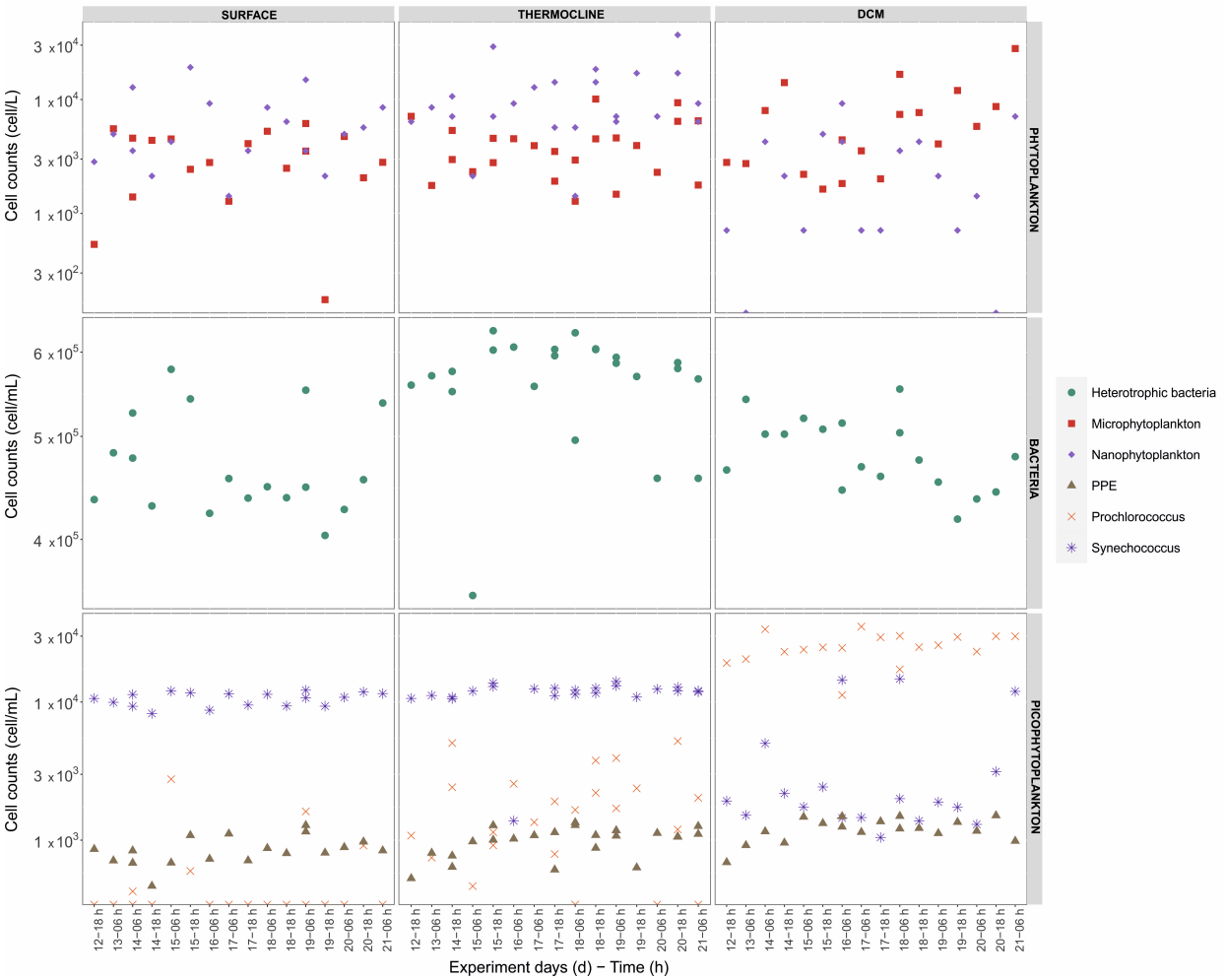

Figure 5. Phytoplankton (micro- and nano-fraction), picophytoplankton (photosynthetic picoeukaryotes, or PPEs, *Synechococcus* sp., and *Prochlorococcus* sp.), and bacterioplankton (heterotrophic bacteria) abundance distribution (surface, thermocline, deep chlorophyll maximum, or DCM, layer) during the investigating period.

3.2.2. Vertical Distributions and Dominant Taxa

Microphytoplankton dominated the DCM layer, while nanophytoplankton contributed most to the thermocline layer (Figure 5). Maximum microphytoplankton and nanophytoplankton abundance was recorded on 21 and 20 July, respectively (Figure 5). Distinct phytoplankton vertical distribution was also observed by CCA ordination (Figure 6) and confirmed as significant using ANOSIM (Supplementary Figure S3).

Dominant taxa, defined as species or groups with maximum abundance >500 cellsL^{-1}, and the frequency of occurrence in samples >50%, were *Cylindrotheca closterium*, *Guinardia flaccida*, *Guinardia striata*, *Hemiaulus chinensis*, *Leptocylindrus danicus*, *Proboscia alata*, *Pseudo-nitzschia delicatissima*, *Rhizosolenia imbricata*, *Thalassionema frauenfeldii*, *Gyrodinium fusiforme*, nano- and micro-scale dinoflagellates, penatae, and nano-scale coccolitophorids (Table 1). The micro-fraction was dominated by diatoms, and *P. delicatissima*, and *T. frauenfeldii* had the

highest maximum abundances, while dinoflagellates, coccolithophorids, and cryptophytes contributed most to the nanophytoplankton (Table 1). The distribution of dominant taxa abundances remained constant throughout the investigating period.

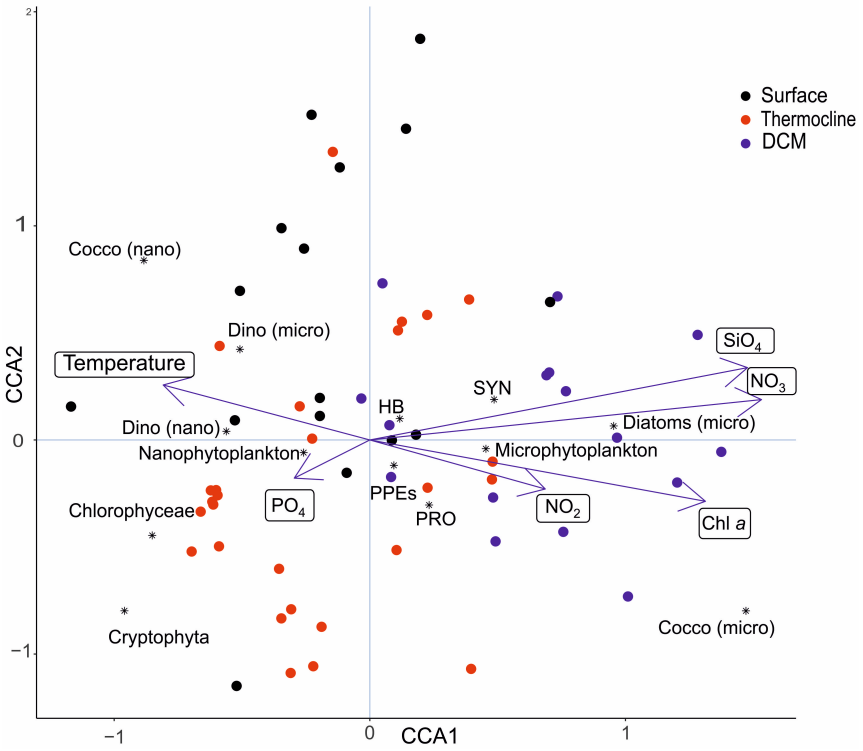

Figure 6. Canonical correspondence analysis (CCA) of environmental variables and plankton groups (pico-, nano-, and microphytoplankton and heterotrophic bacteria). Circles represent sample (N = 59) scores and constraints (weighted averages of plankton groups and linear combinations of constrained variables, respectively) colored by factor water layer (surface, thermocline, and DCM), while asterisk represent scores of plankton groups. Superimposed vectors (arrows) represent explanatory environmental variables: temperature, phosphates (PO_4), nitrates (NO_3), nitrites (NO_2), silicates (SiO_4), and Chl *a*. Abbreviations: PRO (*Prochlorococcus*); SYN (*Synechococcus*); PPEs (photosynthetic picoeukaryotes); HB (heterotrophic bacteria).

Table 1. Maximum abundances (cells L^{-1}) and frequencies of appearance (%) for phytoplankton dominant taxa/groups (dominance is defined as fr > 50%, and max > 500 cells L^{-1}) at station Struga (S1), Lastovo Island, South Adriatic Sea.

Dominant Taxa/Group	Max (Cell L^{-1})	Fr (%)
Dinoflagellates indet. (<20 µm)	23,430	91.67
Penatae indet.	1135	85.00
Pseudo-nitzschia delicatissima (Cleve) Heiden	14,060	81.67
Proboscia alata (Brightwell) Sundström	1325	80.00
Rhizosolenia imbricata Brightwell	755	75.00
Gyrodinium fusiforme Kofoid & Swezy	570	58.33
Coccolitophorids indet. (<10 µm)	5680	55.00
Cylindrotheca closterium (Ehrenberg) Reimann & J.C. Lewin	945	53.33
Leptocylindrus danicus Cleve	3220	53.33
Guinardia flaccida (Castracane) Peragallo	570	51.67
Guinardia striata (Stolterfoth) Hasle	2270	51.67
Hemiaulus chinensis Greville	1135	51.67
Dinoflagellates indet. (micro)	970	51.67
Thalassionema frauenfeldii (Grunow) Tempère & Peragallo	1515	50.00
Cryptophyta	8510	50.00

Average dissimilarity in phytoplankton structure was the highest between the surface and DCM layers (48.9%), where *Thalassionema frauenfeldi* contributed the most. Cryptophyta and nano-scale coccolithophorids contributed the most to the thermocline and DCM layers' dissimilarity (46.47%), while surface and thermocline layer dissimilarity (36.53%) was observed for *Leptocylindrus danicus* and *Pseudo-nitzschia delicatissima*. Cryptophyta, nano-scale coccolithophorids, and nano-scale dinoflagellates contributed the most to overall average dissimilarity in the water column (Table 2).

Table 2. Similarities percentage (SIMPER) analysis of phytoplankton dominant taxa/groups between surface (S), thermocline (T), and deep chlorophyll maximum (DCM) layers, and their contribution to average dissimilarity. Abbreviations: average contribution/standard deviation (δ/σ), species contribution (Σδ%), average dissimilarity (Av. Diss%).

	S and T (δ/σ; Σδ%)	**S and DCM (δ/σ; Σδ%)**	**T and DCM (δ/σ; Σδ%)**
Dominant taxa/groups	Av. Diss% = 36.53	Av. Diss% = 48.86	Av. Diss% = 46.47
Cryptophyta	1.10; 10.2	0.99; 7.49	1.41; 10.58
Coccolitophorids indet. (<10 μm)	1.02; 8.66	1.16; 8.64	1.21; 9.03
Leptocylindrus danicus	1.18; 8.85	1.07; 6.83	1.16; 7.65
Thalassionema frauenfeldi	0.97; 6.54	1.41; 8.09	1.34; 6.99
Cylindrotheca closterium	1.11; 6.45	1.09; 6.05	1.20; 6.61
Guinardia striata		1.30; 7.08	1.45; 7.76
Dinoflagellates indet. (<20 μm)		0.78; 6.71	0.86; 7.04
Proboscia alata		1.19; 6.81	1.15; 6.20
Pseudo-nitzschia delicatissima	1.13; 8.67	1.11; 7.74	
Combried	1.20; 7.58	1.32; 7.35	
Gyrodinium fusiforme	1.20; 6.11		1.57; 7.16
Hemiaulus chinensis	1.21; 6.14		1.14; 5.71
Rhizosolenia imbricate	1.00; 5.96		

3.3. Picophytoplankton and Bacterioplankton

Picophytoplankton was comprised of cyanobacteria *Prochlorococcus* sp. and *Synechococcus* sp., and photosynthetic picoeukaryotes (PPEs). Its specific vertical distribution was observed (Figures 5 and 6) and confirmed to be significant by ANOSIM and PCA (Supplementary Figures S2 and S3C). *Prochlorococcus* sp. and PPEs had the highest abundances in the DCM layer (3.52×10^4 cellmL^{-1} and 1.51×10^3 cellmL^{-1} respectively), while *Synechococcus* sp. dominated in the surface and thermocline layers (maximum abundance of 1.47×10^4 cellmL^{-1} in thermocline layer) (Figure 6, Supplementary Table S6). Heterotrophic bacteria were comprised of high nucleic acid (HNA) and low nucleic acid (LNA) heterotrophic bacteria (HB), and were most active in the thermocline layer where they had maximum abundance of 6.28×10^5 cellmL^{-1} (Figure 6, Supplementary Table S6). Maximum abundances of HNA HB and LNA HB were 3.22×10^5 cellmL^{-1}, and 3.62×10^5 cellmL^{-1}, respectively (Supplementary Table S6). Overall, LNA HB had higher abundance than HNA HB, except in the surface layer, where HNA HB were more abundant (Supplementary Table S6).

3.4. Correlation between Physico-Chemical Parameters and Plankton Community

The highest positive correlations were determined between NO_3 and SiO_4, and NO_2 and PO_4. Chl *a* had a significantly negative correlation with temperature, and significant positive correlations with NO_3 and SiO_4 (Table 3). Observed relationships were confirmed by CCA, indicating different environments in the stratified water column (Figure 6).

Environmental variables significantly explained 18.3% of phytoplankton and bacterioplankton variability ($p = 0.003$), while the most significant effect was in the CCA1 axis ($p = 0.001$) (Supplementary Table S7). NO_3, NO_2, and SiO_4 were positively correlated with the CCA1 axis, while temperature and PO_4 were negatively correlated (Supplementary Table S7). Samples represented as weighted averages of species and linear combinations of

constrained variables tend to cluster according to water column stratification into surface water, thermocline, and DCM groups, therefore, elucidating a distinct plankton vertical distribution and significant nutrient gradient, as shown in Figure 6. The CCA indicated heterotrophic bacteria, PPEs, *Prochlorococcus*, nanophytoplankton, and micro-scale dinoflagellates to have a niche in the surface and thermocline layers, while *Synechococcus*, microphytoplankton, and micro-scale diatoms had a trend of linear increase towards the DCM layer (Figure 6). Furthermore, CCA showed that temperature, NO_3, and SiO_4 were the main factors influencing the vertical distribution and abundances of phytoplankton and bacterioplankton.

Table 3. Spearman's rank order correlation matrix for physico-chemical parameters. Only significant correlations are shown ($p < 0.05$, N = 59) Only significant correlations are shown ($p < 0.06$, N = 59). Bold values represent the highest correlations for each parameter.

	NO_2	**NO_3**	**PO_4**	**SiO_4**	**Temp**	**Chl *a***
NO_2 (μM)	1.00					
NO_3 (μM)	0.45	1.00				
PO_4 (μM)	0.63	0.65	1.00			
SiO_4 (μM)	0.37	0.85	0.56	1.00		
Temperature (°C)		0.53		−0.42	1.00	
Chlorophyll *a* (μgL^{-1})		0.57		0.50	−0.74	1.00

3.5. Plankton Community Composition Revealed through HTS

The prokaryotic plankton community revealed by high-throughput sequencing (HTS) was dominated by Proteobacteria (41–73%), Bacteroidota (9.5–27%) and cyanobacteria (1–10%; higher relative abundances in pico- and nano-fractions sampled at the beginning of the study period in the DCM) (Figure 7A). Proteobacteria are equally represented with alphaproteobacteria (relative abundancy alternated) and gammaproteobacteria (increased in relative abundancy towards the end of investigating period). Planctomycetota (1–15%) had the highest values in the DCM layer nano-fraction sampled at the beginning of the experiment (Figure 7A). Surface water samples had higher relative abundances of Verrucomicrobiota at both beginning and end of the experiment (5% and 9%, respectively). Firmicutes and Marinimicrobia were generally less represented in samples (the highest relative abundances of Firmicutes were in the micro-fraction surface sample at the end of the study period (~6.5%), while Marinimicrobia had ~5% in the pico-fraction at DCM and surface layers, at the beginning and end of experiment, respectively. Differences between fractions are most prominent between the pico- versus micro-fraction (Supplementary Table S2, Shannon diversity index for the 16S rRNA gene).

The eukaryotic plankton community as determined by amplicon sequencing of the 18S rRNA gene after filtering out metazoan sequences (fragments of crustacean skeletons or higher mesozooplankton), mitochondria, chloroplast, and unassigned sequences is shown through relative abundance bar plots as a phylum-ranked taxonomy and order-ranked heatmap (Figure 7B). In congruence with microscopy abundances, the eukaryotic plankton community was composed of dinoflagellates of which the majority represent parasitic Syndiniales (45–80%), followed by Stramenopiles (Ochrophyta; 2–18%), Ciliophora (of which the majority are parasitic Spirotrichea; 2–21%), chlorophytes (2–4%), and haptophytes (1–4%). Phyllum Ochrophyta dominated with diatoms (Bacillariophyta; 1–13%), while a significant proportion of samples also showed the phyla Pelagophyta (0.5–12%) and Chrysophyta (0.5–3%). Class Prymnesiophyceae dominates in phyllum Haptophyta with an average of 0.5–3.5%, while cryptophytes comprise only 0.3–1% of assemblages throughout all samples (Figure 7B).

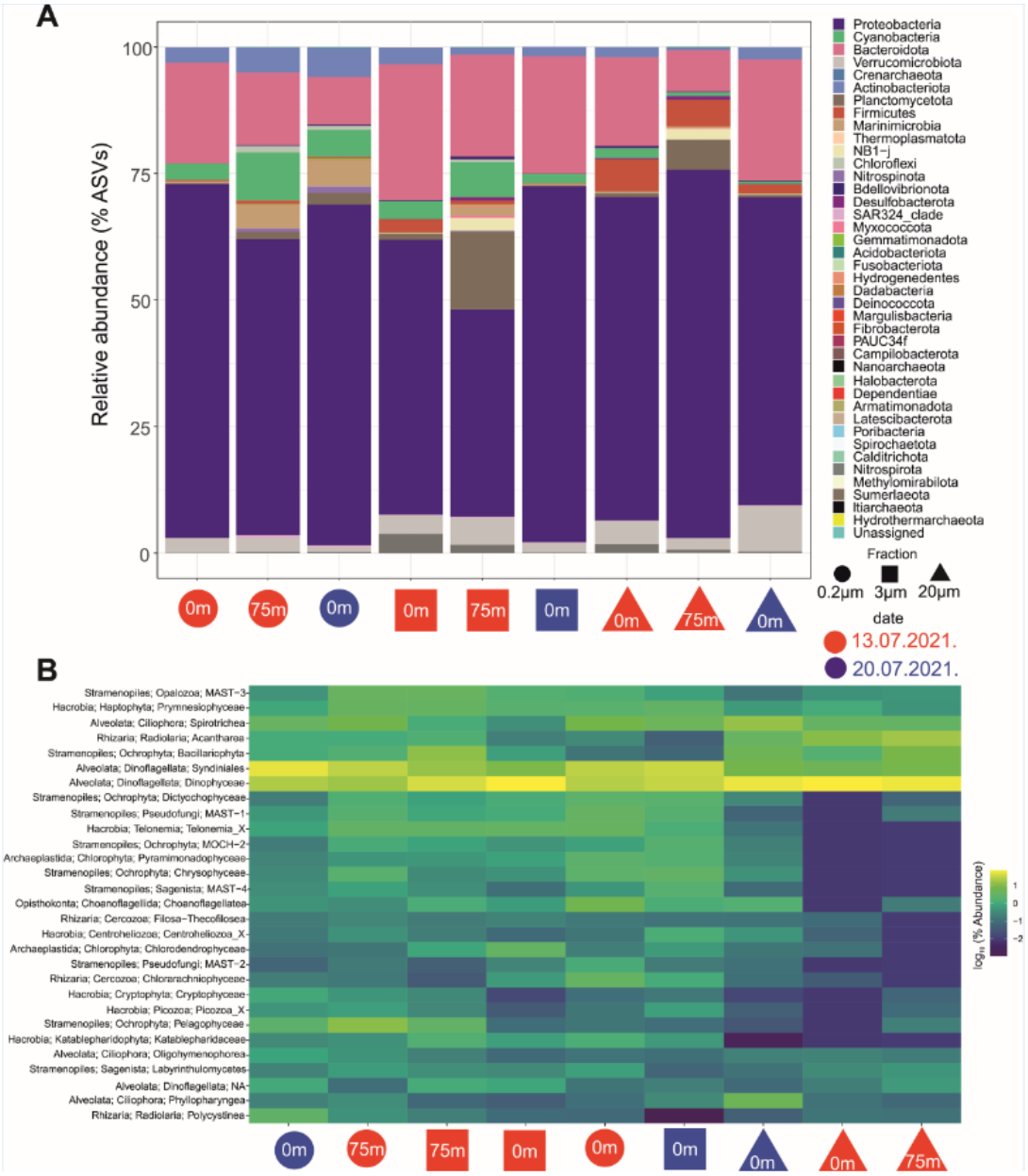

Figure 7. (**A**) Bar plot with relative abundances (ASV%) in the prokaryotic community, phylum level. (**B**) Heatmap with relative abundances ($\log_{10}$ ASV%) in eukaryotic community, phylum level. Legend explaining symbols of fractioned samples and colors of sample dates positioned in the bottom right corner of panel A.

Differences between the fractions (pico-, nano-, and micro-) were most prominent between pico- and nano-fractions versus micro-fractions (Figure 7). The micro-fraction was generally less diverse (Supplementary Table S2, Shannon diversity index for the 18S rRNA gene), containing significantly more radiolarian and dinoflagellate sequences, while in smaller fractions the diversity increases with Ochropyta and Chlorophyta increasing in ASV frequencies (Figure 7B).

The cladogram with adjacent ASV frequencies showing the microscopy relevant 211 taxa is presented in Figure S3. The most frequent taxa belong to the dinoflagellate genus *Gyrodinium* within the nano-fraction collected at the beginning of the experiment, while the most frequent dinoflagellate genus within the pico-fraction was *Amphidinium*, detected at the end of the experiment. The most frequent diatoms were pennate genera *Pseudo-nitzschia* (highest ASV frequencies detected at DCM at the beginning of the ex-

periment) and multipolar centric *Chaetoceros*, which had slight peak in ASV frequency in the pico-fraction DCM layer sample collected at the beginning of the experiment (Supplementary Figure S1). Chlorophyta were represented with omnipresent genera, such as *Ostreococcus*, *Bathycoccus*, *Pycnococcus*, *Mamiella*, *Pterosperma*, and *Halosphaera*, while Haptophyta sequences were identified mostly as class Chrysochromulinaceae or Phaeocystaceae (Supplementary Figure S1).

4. Discussion

4.1. Nutrients and Thermal Stratification

The South Adriatic Sea is characterized by relatively low phosphate and nitrate concentrations (generally less than 0.2 μmol L^{-1}, and 3 μmol L^{-1}, respectively), and primary production is often limited by phosphate [42,43]. However, during winter mixing and enhanced river inflow, nitrate can reach maximum values of 2.5 μmol L^{-1} in offshore areas [42] and up to 14–20 μmol L^{-1} in eutrophic estuaries [44]. The nutrient concentrations recorded in the Lastovo archipelago (Figure 3) are, therefore, in congruence with previous studies and with oligotrophic stratified ecosystems. However, extremes recorded at the beginning of the study period with values of 10.3 μmol L^{-1}, 0.76 μmol L^{-1}, and 3.53 μmol L^{-1} for NO_3, PO_4, and SiO_4 (Figure 3), respectively, are more typical for eutrophic systems, such as the Neretva Estuary (11.6 μmol L^{-1}, 0.81 μmol L^{-1}, and 13.9 μmol L^{-1}—averaged annual values for NO_3, PO_4, and SiO_4, respectively [45]), Mali Ston Bay (9.73 μmol L^{-1}, 0.33 μmol L^{-1}, and 6.24 μmol L^{-1} [46]), and Boka Kotorska Bay (9.92 μmol L^{-1}, 0.581 μmol L^{-1}, and 14.0 μmol L^{-1} [47]). Furthermore, maximum values for NO_3, PO_4, and SiO_4 measured in the Eastern Mediterranean are 9.011 μmol L^{-1}, 0.381 μmol L^{-1}, and 10.660 μmol L^{-1}, respectively [48]. Therefore, we can discuss the extremes at Lastovo Island as indicators of nutrient influx to the euphotic layer during thermal stratification.

Stratification in the southern Adriatic Sea generates a thermocline in April and culminates in August [43], with temperatures above the thermocline being between 22 °C and 26 °C [49], as observed with our temperature data loggers (Figure 2). The maximum Chl *a* concentration recorded at Lastovo Island was 0.2 μg L^{-1} in the DCM layer at 65–75 m, which coincided with higher SiO_4 and NO_3 concentrations and microphytoplankton abundances. Thermal stratification at Otranto Strait was recorded in the layer between 10 and 50 m with maximum Chl *a* concentrations being between 0.17–1.1 μg L^{-1} [50,51]. Chl *a* and temperature showed significant negative correlations, while Chl *a*, NO_3, and SiO_4 showed significant positive correlations, which indicated the DCM (Table 3) [51–54].

4.2. Phytoplankton Community in the Oligotrophic Ecosystem

Contrary to the northern Adriatic Sea, the oligotrophic southern Adriatic Sea is characterized by low phytoplankton abundances with maximum abundances occurring in spring [42,49]. Nanophytoplankton and microphytoplankton abundances (36.9×10^3 cells L^{-1} and 28×10^3 cells L^{-1}, respectively) (Figure 5) are characteristic for the South Adriatic Sea [43,51,53,55] and oligotrophic Mediterranean Sea [56–60]. In the stratified South Adriatic Sea, microphytoplankton abundances range between 49.2×10^3 cells L^{-1} in open sea areas [43], 21.3×10^5 cells L^{-1} in bays [46], and up to 7.9×10^6 cells L^{-1} in karstic estuaries [45], while offshore nanophytoplankton abundances are between 1.1×10^5 cells L^{-1} and 1.5×10^5 cells L^{-1} [42]. In general, ecosystems rich in inorganic nutrients will support microphytoplankton, while organic nutrients are preferred by nano- and picophytoplankton [51,61]. Diatoms, one of the main constituents of microphytoplankton, rapidly respond to higher nitrate concentrations and outcompete other phytoplankton [62] which may explain their development in the DCM layer. Diatoms dominating microphytoplankton, and dinoflagellates dominating the nanophytoplankton community (Figure 4), are characteristic for the South Adriatic Sea [9,44,46,63,64]. In the oligotrophic Mediterranean Sea they thrive only in areas of nutrient inflow increase, and picophytoplankton dominates [65].

Nano-scale dinoflagellates were the most dominant taxa (Table 1), which is supported by records of nano-scale dinoflagellates and coccolithophorids being more frequent than

micro-scale diatoms in the stratified Mediterranean Sea [66] and in the Adriatic Sea [67]. In addition, HTS results recognize dinoflagellates over diatoms as the main contributors to the plankton community, of which most reads are annotated to parasitic Syndiniales (Figure 7B). This can be explained with multiple copies of dinoflagellate genomes [68] and/or PCR biases in the metagenomic amplicon sequencing approach [69]. The prevalence of sequences of these, for hosts, fatal parasites, are shown in all major oligotrophic oceans and seas, including the Mediterranean [70] and Adriatic Sea [71] especially within the smallest size-fraction (<5 μm) [72].

4.2.1. Microphytoplankton

Of the micro-scale diatoms revealed by light microscopym *Pseudo-nitzschia delicatissima*, *Proboscia alata*, *Rhizosolenia imbricata*, and *Thalassionema frauenfeldii* were most abundant in more than 50% of samples (Table 1). *Pseudo-nitzschia* spp., *Proboscia alata*, and *Rhizosolenia* spp. were also identified among the 18S rRNA ASVs (Figure S3), of which *Pseudo-nitzschia* spp. contributed the most, confirming its dominance among diatoms within this study. Other (multipolar) centrics identified among the 18S rRNA ASVs predominantly belonged to genus *Chaetoceros* (species: *Ch. diversus*, *Ch. throndsenii*, *Ch. decipiens*, *Ch. vixvisibilis*, *Ch. anastomosans*, *C. lauderi*, *Ch. socialis*, *Ch. tortissimus*, and *Ch. curvisetus*), followed by *Minidiscus*, *Thalassiosira*, *Leptocylindrus*, and *Hemiaulus*, which is congruent with Piredda et al., 2018 [73], who showed the dominance of *Chaetoceros–Leptocylindrus–Thalassiosira* assemblages in coastal European seas.

Pseudo-nitzschia spp. is described to be distributed across the Adriatic Sea and frequent in all seasons [74], but is also characteristic for nutrient enriched ecosystems [74–76]. A similar diversity was observed in other studies in the South Adriatic Sea, with *Pseudo-nitzschia delicatissima*, *Pseudo-nitzschia* spp., *Leptocylindrus danicus*, *Proboscia alata*, *T. frauenfeldii*, and *Thalassionema nitzschioides* often being dominant diatoms [43,46,51,77]. In general, it is recorded that centric diatoms characterize the South Adriatic Sea, in contrast to pennatae diatoms that are more frequent in the North Adriatic Sea [49]. Dominant diatom species often found in the DCM in the Mediterranean Sea are *Dactyliosolen fragilissimus*, *Pseudo-nitzschia* sp., *Pseudo-nitzschia delicatissima*, *Rhizosolenia* sp., *Thalassiosira* sp., *Thalassionema nitzschioides*, *Th. frauenfeldii*, *Leptocylindrus danicus*, *Bacteriastrum* sp., and *Hemiaulus* sp. [78–80]. These findings are consistent with observed diatom assemblage in the Lastovo archipelago (Table S3) that can be described as part of the *Chaetoceros–Rhizosolenia* (*Proboscia*) community characteristic of the eastern Adriatic and Mediterranean and which often includes the following genera: *Chaetoceros*, *Pseudo–nitzschia*, *Proboscia*, *Rhizosolenia*, *Bacteriastrum*, *Cerataulina*, *Leptocylindrus*, and *Thalassionema* [50,81,82]. Differences in diatom composition in the northern and southern Adriatic can be explained with the nitrogen availability, since the availability of nitrogen can be a driver of development and abundance of different diatom species [83].

4.2.2. Nanophytoplankton

Nanophytoplankton was dominated by dinoflagellates, coccolithophorids, and cryptophytes (Table 1), which is in accordance with previous studies of the South Adriatic [47,54,84,85], and Mediterranean Sea [80,86,87].

Frequent dinoflagellate genera in the South Adriatic Sea are *Dinophysis*, *Gonyaulax*, *Gymnodinium*, *Oxytoxum*, *Prorocentrum*, *Protoperidinium*, and *Tripos* [43,46,47,88], of which only a few were recorded in the Lastovo archipelago (Supplementary Table S4). In the Mediterranean Sea, frequently observed taxa are *Gymnodinium*, *Gyrodinium*, *Tripos*, *Protoperidinium*, and *Oxytoxum* [89–91], all of which were observed at Lastovo Island (except *D. fortii*), but not frequently (Supplementary Table S4). Common coccolithophorid species observed in South Adriatic Sea are *Calyptosphaera oblonga*, *Calciosolenia brasilliensis*, *Emiliana huxley*, *Helicosphaera walichii*, *Rhabosphaera tignifera*, and *Syracosphaera pulchra* [92]. The coccolithophorid community is also highly diverse in the Mediterranean Sea, and *Emiliania huxleyi* is an often dominant and widespread species [93]. A similar community was

found at Lastovo Island, except *H. walichii* and *R. tignifera* (Supplementary Table S4). The silicoflagellate species *Dictyocha fibula* was also recorded in studies of the South Adriatic Sea phytoplankton community [47], and in the Mediterranean Sea where it is scarce and mostly found in surface layers [94,95].

The bias of comparing taxa lists obtained by different observers/taxonomers should be considered, as well as seasonality, sampling location, and the different methodologies used, as shown in the more diverse dinoflagellate community revealed by HTS vs. microscopy. Some genera were recorded only via the 18S rRNA ASVs: *Ceratoperidinium*, *Karlodinium*, *Azadinium*, *Lepidodinium*, *Blastodinium*, *Heterocapsa*, *Karenia*, *Torodinium*, *Biecheleria*, *Pelagodinium* etc., all of which were reported previously in the South Adriatic [71] and in other coastal marine areas [73,96–98]. Relative abundances of ASVs belonging to dinoflagellate genera revealed their dominance in the phytoplankton community, especially *Gyrodinium*, which was dominant in reads in all samples, with the highest number observed in the surface pico-fraction collected at the beginning of experiment (13 July 2021) (Supplementary Figure S1). In general, smaller fractions, such as pico-nano cell sizes, mostly accumulate the classes Dinophyceae and other MALVs (marine alveolates, mostly parasitic), followed by *Rhizaria* and *Stramenopiles* [68,99]. Within haptophytes, HTS data associated most ASVs to *Chrysochromulina*, *Phaeocystis*, *Prymnesium*, *Haptolina*, *Algirosphaera*, *Helicosphaera*, and *Syrachosphaera*, while the rest of the reads belonged to Haptophyta_Clades HAP4 and HAP5. Interestingly, there were no *E. huxley* ASVs in our dataset, nor was it recorded via light microscopy, which can be corroborated with the findings of Piredda et al., 2017 [70] and Gran-Stadniczeñko et al., 2019 [95]. They noted that higher abundances of *Emiliania huxley* regarding the V4 region of the 18S rRNA gene are expected in late summer and fall in coastal seas [98,100], allowing us to conclude that the period of our experiment was not favorable for *E. huxley* growth.

4.3. Phytoplankton Vertical Distribution

Significant distinct phytoplankton vertical distribution was driven by temperature and nutrients (Figure 6). Cryptophytes, nano-scale coccolithophorids, and dinoflagellates contributed the most to the statistically significant dissimilarity between surface, thermocline, and DCM layers (Table 2). Dinoflagellates and diatoms' opposite responses to temperature are observed in other studies [54], which can be explained by dinoflagellates having their temperature optima higher than 24 °C, while diatoms are most abundant in bottom layers where temperature is between 16 °C and 24 °C [46]. Furthermore, there is a tendency of the microphytoplankton community sinking to the bottom layers towards the end of summer [53,77]. Similar significant vertical distribution is also recorded in studies of the stratified Mediterranean Sea [65,99] where the community in the DCM is often comprised of diatoms [79,101] and picoplankton, specifically *Prochlorococcus* [56,102,103], while *Synechococcus* thrives in the surface layer [48,104]. Although we did not observe temperature as a significant constraint for picophytoplankton and bacterioplankton (Figure 6), the neural network analysis study revealed positive correlation of PPEs, cyanobacteria, and heterotrophic bacteria with temperature in the oligotrophic South Adriatic [102].

A common trend of linear increase is evident for NO_2 concentration, microphytoplankton, and micro-scale diatom abundances (Figure 6). TIN (total inorganic nitrogen) was eliminated from the CCA as a highly correlated variable with NO_2 (calculated using variance inflation factors test) which is, therefore, its proxy. As a result, we can discuss TIN as an influential factor in phytoplankton community diversity [45], which is in accordance with previously observed high microphytoplankton abundances in areas rich with inorganic nutrients, while nanophytoplankton thrives in layers where organic nutrients are formed [51,61,105]. Nano-scale groups followed an inverse trend with nutrients (Figure 6), which indicates a preference for low-nutrient environments. Such nutrient–phytoplankton correlations were confirmed by other studies in the oligotrophic South Adriatic Sea [45,54,97], and the Mediterranean Sea [99,105,106].

4.4. Picophytoplankton and Heterotrophic Bacteria

Picophytoplankton tends to dominate the photosynthetic biomass in the oligotrophic Mediterranean Sea [96]. The cyanobacteria distribution is constant [107], while picoeukaryotes are frequently observed in the Ionian Sea, Strait of Sicily, and the Levantine Basin [65]. The community at Lastovo Island was comprised of the cyanobacteria *Prochlorococcus* sp. and *Synechococcus* sp., and PPEs (Figure 5). *Prochlorococcus* and *Synechococcus* abundances (10^3 to 10^4 cell mL^{-1}, Figure 5) are typical for the oligotrophic South Adriatic open sea regions [103,108], and for the Mediterranean Sea [109–111]. *Synechococcus* was more successful in the surface and thermocline layers, while *Prochlorococcus* peaked in the DCM (Figure 5). The observed distinct niches of *Prochlorococcus* and *Synechococcus* are characteristic for oligotrophic waters [112,113], and are often recorded in the South Adriatic [4,8,114], and the Mediterranean Sea [87], Temperature and nutrients are important factors determining their distribution [4,109,115–117], especially *Synechococcus*, which easily adapts to different temperatures and nutrient sources [104,118].

Prochlorococcus and *Synechococcus* were also identified as photosynthetic counterparts of bacterial ASVs congruently to previous studies within the same area [26,71,119]. However, in those studies, Cyanobacteria relative OTUs abundance in the winter were higher compared to our results [26,71]. Nevertheless, as it was observed by Korlević et al., 2015 [119] that an unusually strong winter deep convection event adds up to those higher relative abundancies, question of methodology used (454-pyrosequencing along with classification to OTUs instead of ASVs in post-bioinformatic analysis of raw reads) should be considered.

PPEs' abundance follows the trend of increased NO_2 and PO_4 concentrations (Figure 6), which confirms they are very successful in ecosystems with elevated nutrient levels [116]. Their abundance remained constant throughout the water column (Figure 5). Maximum abundance was recorded in the DCM layer (Table S5), which is congruent with other studies carried out in the Mediterranean in summer [99] and in the Adriatic Sea in spring [114,120]. Due to their size and lack of distinguishing characters, most PPE cells are overlooked in traditional monitoring by light-microscopy studies [121]. Therefore, the importance of sequencing that fraction arose with global expeditions, such as the Biosope and Tara Oceans [100,122], which showed that most PPEs belong to the classes Prymnesiophyceae, Prasinophyceae, Mamiellophyceae, Cryptophyceae, Pelagophyceae, Chrysophyceae, and Dictyochophyceae [123]. Heterotrophic counterparts of pico-nano size-fractions as confirmed within this study are mostly bacterivorous (alveolates and stramenopiles) and play a key role in nutrient recycling [124] and community control through predation pressure or parasitism [117].

High bacterial activity in the nutrient-poor surface and thermocline layers (Supplementary Table S6, Figure 3) was confirmed by HNA and LNA HB maximum abundances (Supplementary Table S6) characteristic of the oligotrophic South Adriatic Sea in summer (10^4–10^5) [102,103,114]. The increase in bacteria in the surface layer of the stratified South Adriatic Sea [4,114,125,126] can be explained by nutrient utilization in the productive surface layers (low nutrients and high bacteria abundances), and nutrient regeneration and accumulation in deeper layers (high nutrient and low bacteria abundances) [4]. LNA HB had higher abundances than HNA HB (Supplementary Table S6), often observed in the South Adriatic Sea [26,114] because LNA HB are dominated by the alphaproteobacterial group SAR11 which prefers oligotrophic waters [26,114] and is well adapted to low nutrient concentrations [103].

The microbial community at Lastovo Island was comprised mostly of Proteobacteria, represented by Alphaproteobacteria and Gammaproteobacteria, followed by Bacteroidota and Cyanobacteria (Figure 7A). Šantić et al., 2021 [102] neural network analysis revealed similar dominance of Proteobacteria in the oligotrophic South Adriatic Sea, followed by Bacteroideota and Actinobacteriota, which were not observed in high relative abundances at Lastovo Island (Figure 7A). HTS revealed dynamic vertical distribution of the bacterial community, with Marinmicrobia being more frequent in DCM and surface layers at the

beginning and end of the experiment, respectively (Figure 7A). Verrucomicrobiota had higher relative abundances at the surface layer, while Planctomycetota had the highest values in the DCM layer (Figure 7A). Similarly, the San Pedro Ocean Time series study (2005–2018) revealed prokaryotic community diversity that has steady dynamics and is vertically distinct [127]. The euphotic zone is dominated by Rhodobacterales, SAR86, and Puniceispirillales (SAR116) that represent the small size-fraction, with Synechococcales, Actinomarinales, Cellvibrionales dominating the large size-fraction. Deeper layers are dominated by Nitrosopumilales Archaea, Thiomicrospirales, Nitrospinales, Marinimicrobia, and SAR234 predominated, all representing small size-fraction [127].

There are numerous case studies confirming the HTS method to add to the value of investigating plankton community diversity [128]. For example, it elucidated that the most diverse and dominant diatom genus in the plankton is *Chaetoceros* with over 200 validated species. Light microscopy is limited in identifying species by morphological characteristics only, while HTS can help identify rare and cryptic species [73,100]. However, the HTS method has disadvantages, such as bias in choosing the marker region, no universally accepted gene for algae barcoding, presence of intros, etc. [128]. Therefore, combining HTS metabarcoding and light microscopy methods yields valuable results on phytoplankton and bacterioplankton community diversity, and both were used to examine phytoplankton and bacterioplankton diversity and co-dependency at Lastovo Island.

5. Conclusions

Diatoms and dinoflagellates contributed the most to micro- and nanophytoplankton, respectively, while the pico-fraction comprised of PPEs and the cyanobacteria *Synechococcocus* sp. and *Prochlorococcus* sp. Bacterioplankton comprised of HNA and LNA heterotrophic bacteria, and the main prokaryotic groups revealed by HTS were Proteobacteria, Bacteroidota, and cyanobacteria. Differences in pico-, nano-, and microphytoplankton community diversity were most prominent between pico- and nano-fractions versus the micro-fraction, which was generally less diverse. Temperature vertical profiles, correlations between nutrients, Chl *a*, and temperature, and overall nutrients and Chl *a* concentration indicated a stratified water column. In addition, phytoplankton and bacterioplankton community vertical distribution additionally supported dissimilarity between surface, thermocline, and DCM layers. Cryptophytes, nano-scale coccolithophorids, and nano-scale dinoflagellates contributed the most to this distinction, as they were most frequent and abundant, which is typical for the oligotrophic South Adriatic Sea ecosystem. However, the dominant diatoms *Pseudo-nitzschia delicatissima*, *Proboscia alata*, *Rhizosolenia imbricata*, and *Thalassionema frauenfeldii* (present in more than 50% of samples in high numbers) can be indicators of a nutrient-enriched area. In addition, nutrient extremes observed at the beginning of the study period are unusual for the stratified and oligotrophic South Adriatic Sea ecosystem in summer, therefore, indicating a possible nutrient flux to the euphotic layer that could affect the observed phytoplankton community diversity.

Supplementary Materials: The following supporting information can be downloaded at: https://www.mdpi.com/article/10.3390/w15122299/s1, Figure S1: Cladogram with adjacent ASV frequencies showing microscopy relevant 211 taxa. Cladogram was constructed using plugin q2-phylogeny, MAFFT program, and FastTree, and visualized using iTOL 4.4.2. Taxonomy dataset generated in QIIME2 using PR2 database was added to the cladogram, representing 211 relevant taxa spread through Dinophyta, Cryptophyta, Haptophyta, Chlorophyta, and Bacillariophyta. Sample frequency (number of ASVs identified as individual representative sequences) was added using FeatureTable; Figure S2: Principal component analysis (PCA) of environmental variables with overlaid vectors whose direction and length indicate negative or positive correlations of abiotic variables with PC1 and PC2 axes.; Figure S3: Analysis of similarities (ANOSIM) test confirming: (A) significant nutrient concentration decrease after 16 July 2021, (B) significant nutrient gradient with distinct concentrations between surface, thermocline and deep chlorophyll maximum layer, (C) significant vertical distribution of nano-, micro-, picophytoplankton, and bacterioplankton; Table S1: Sampling categories with corresponding sampling depths at station Struga (S1) (N 42.72285, E 16.88676) during

investigating period. Abbreviations: DCM (deep chlorophyll maximum); Table S2: eDNA samples (Station-depth-fraction-date) with numbers of raw input reads, filtrated, denoised, and non-chimeric reads.; Table S3: Principal component analysis (PCA) of environmental variables showing loadings (eigenvectors) of environmental variables, with highest values highlighted, and cumulative variability explained by PC1 and PC2 axes with corresponding eigenvalues; Table S4: List of groups/taxa determined by the Utermöhl method from samples taken at station Struga (S1) at Lastovo Island in the Adriatic Sea, with corresponding maximum abundances (cell L^{-1}), minimum abundances (cell L^{-1}), and frequency of appearance in samples (%). The total number of samples is 60. Abbreviations: Min (minimum abundances), Max (maximum abundances), Fr (frequency of appearance), N.D (not determined); Table S5: Phytoplankton community biodiversity indices at station Struga (S1), Lastovo Island, South Adriatic. Abbreviations: S (total species number), N (total number of individuals), d (species richness), J′ (Pielou's evenness), H′ (Shannon–Weiner diversity), $1 - \lambda$ (species diversity); λ (Simpson's Index); Table S6: Maximum bacterioplankton and picophytoplankton abundance determined by flow cytometry. Abbreviations: Max (maximum abundance), HB (heterotrophic bacteria), HNA HB (high nucleic acid heterotrophic bacteria), LNA HB (low nucleic acid heterotrophic bacteria), PRO (*Prochlorococcus*), SYN (*Synechococcus*), PPEs (Photosynthetic picoeukaryotes).; Table S7: Canonical correspondence analysis (CCA) results showing percentage of variability explained by constrained and unconstrained axes, eigenvalues for constrained axes and ANOVA permutation test results (F and *p* value) for entire model and for constrained axis.

Author Contributions: Conceptualization, Z.L. and A.M.; methodology, Z.L., H.Č. and H.M.; software, H.M. and A.M.; validation, H.M. and V.C.; formal analysis, Z.L., M.M., R.C., A.C.T. and E.P.A.; investigation, Z.L., H.Č., B.Č. and V.C.; resources, Z.L., E.P.A., H.Č. and R.C.; data curation, Z.L.; writing—original draft preparation, Z.L. and A.M.; writing—review and editing, Z.L., A.M., E.P.A., M.M., V.C., R.C., A.C.T. and H.M.; visualization, A.M. and H.M.; supervision, Z.L.; project administration, Z.L. and V.C.; funding acquisition, Z.L. and V.C. All authors have read and agreed to the published version of the manuscript.

Funding: This work was funded by Croatian Science Foundation under the projects ISLAND (IP-2020-02-9524) and METALPATH (lP-2019-04-5832).

Data Availability Statement: Not applicable.

Acknowledgments: We thank the captain and crew of the R/V Baldo Kosić II, Marine Explorers Society 20.000 leagues team, and Rade Garić, Marta Žižek, and Tomislav Zetović, who made this research possible.

Conflicts of Interest: The authors declare no conflict of interest.

References

1. Field, C.B.; Behrenfeld, M.J.; Randerson, J.T.; Falkowski, P. Primary Production of the Biosphere: Integrating Terrestrial and Oceanic Components. *Science* **1998**, *281*, 237–240. [CrossRef]
2. Kirchman, D.L. *Microbial Ecology of the Oceans*; John Wiley & Sons: Hoboken, NJ, USA, 2000; ISBN 978-0-471-29992-9.
3. Viličić, D. *Ecology and Composition of Phytoplankton in the Adriatic Sea*; Koeltz Scientific Books: Koenigstein, Germany, 2014; ISBN 978-3-87429-474-4.
4. Najdek, M.; Paliaga, P.; Šilović, T.; Batistić, M.; Garić, R.; Supić, N.; Ivančić, I.; Ljubimir, S.; Korlević, M.; Jasprica, N.; et al. Picoplankton Community Structure before, during and after Convection Event in the Offshore Waters of the Southern Adriatic Sea. *Biogeosciences* **2014**, *11*, 2645–2659. [CrossRef]
5. Babić, I.; Petrić, I.; Bosak, S.; Mihanović, H.; Dupčić Radić, I.; Ljubešić, Z. Distribution and Diversity of Marine Picocyanobacteria Community: Targeting of Prochlorococcus Ecotypes in Winter Conditions (Southern Adriatic Sea). *Mar. Genom.* **2017**, *36*, 3–11. [CrossRef]
6. Gačić, M.; Civitarese, G.; Miserocchi, S.; Cardin, V.; Crise, A.; Mauri, E. The Open-Ocean Convection in the Southern Adriatic: A Controlling Mechanism of the Spring Phytoplankton Bloom. *Cont. Shelf Res.* **2002**, *22*, 1897–1908. [CrossRef]
7. Batistić, M.; Jasprica, N.; Carić, M.; Čalić, M.; Kovačević, V.; Garić, R.; Njire, J.; Mikuš, J.; Bobanović-Ćolić, S. Biological Evidence of a Winter Convection Event in the South Adriatic: A Phytoplankton Maximum in the Aphotic Zone. *Cont. Shelf Res.* **2012**, *44*, 57–71. [CrossRef]
8. Cerino, F.; Bernardi Aubry, F.; Coppola, J.; La Ferla, R.; Maimone, G.; Socal, G.; Totti, C. Spatial and Temporal Variability of Pico-, Nano- and Microphytoplankton in the Offshore Waters of the Southern Adriatic Sea (Mediterranean Sea). *Cont. Shelf Res.* **2012**, *44*, 94–105. [CrossRef]

9. Ljubimir, S.; Jasprica, N.; Čalić, M.; Hrustić, E.; Dupčić Radić, I.; Car, A.; Batistić, M. Interannual (2009–2013) Variability of Winter-Spring Phytoplankton in the Open South Adriatic Sea: Effects of Deep Convection and Lateral Advection. *Cont. Shelf Res.* **2017**, *143*, 311–321. [CrossRef]
10. Vilibić, I.; Matijević, S.; Šepić, J.; Kušpilić, G. Changes in the Adriatic Oceanographic Properties Induced by the Eastern Mediterranean Transient. *Biogeosciences* **2012**, *9*, 2085–2097. [CrossRef]
11. Lučić, D.; Ljubešić, Z.; Babić, I.; Bosak, S.; Cetinić, I.; Vilibić, I.; Mihanović, H.; Hure, M.; Njire, J.; Lučić, P.; et al. Unusual Winter Zooplankton Bloom in the Open Southern Adriatic Sea. *Turk. J. Zool.* **2017**, *41*, 1024–1035. [CrossRef]
12. Hure, M.; Mihanović, H.; Lučić, D.; Ljubešić, Z.; Kružić, P. Mesozooplankton Spatial Distribution and Community Structure in the South Adriatic Sea during Two Winters (2015, 2016). *Mar. Ecol.* **2018**, *39*, e12488. [CrossRef]
13. Mihanović, H.; Orlić, M.; Pasarić, Z. Diurnal Thermocline Oscillations Driven by Tidal Flow around an Island in the Middle Adriatic. *J. Mar. Syst.* **2009**, *78*, S157–S168. [CrossRef]
14. Mihanović, H.; Beg Paklar, G.; Orlić, M. Resonant Excitation of Island-Trapped Waves in a Shallow, Seasonally Stratified Sea. *Cont. Shelf Res.* **2014**, *77*, 24–37. [CrossRef]
15. Hogg, N.G. Observations of Internal Kelvin Waves Trapped Round Bermuda. *J. Phys. Oceanogr.* **1980**, *10*, 1353–1376. [CrossRef]
16. Brink, K.H. Island-Trapped Waves, with Application to Observations off Bermuda. *Dyn. Atmos. Ocean.* **1999**, *29*, 93–118. [CrossRef]
17. Luther, D.S. Trapped Waves around the Hawaiian Islands. In Proceedings of the 3rd 'Aha Huliko' a Hawaiian Winter Workshop, Hawaiian Ocean Experiment, Honolulu, HI, USA, 21–24 January 1985; pp. 261–301.
18. Merrifield, M.A.; Yang, L.; Luther, D.S. Numerical Simulations of a Storm-Generated Island-Trapped Wave Event at the Hawaiian Islands. *J. Geophys. Res. Ocean.* **2002**, *107*, 33-1–33-10. [CrossRef]
19. Pizarro, O.; Shaffer, G. Wind-Driven, Coastal-Trapped Waves off the Island of Gotland, Baltic Sea. *J. Phys. Oceanogr.* **1998**, *28*, 2117–2129. [CrossRef]
20. Lazure, P.; Le Cann, B.; Bezaud, M. Large Diurnal Bottom Temperature Oscillations around the Saint Pierre and Miquelon Archipelago. *Sci. Rep.* **2018**, *8*, 13882. [CrossRef] [PubMed]
21. Mihanović, H.; Orlić, M.; Pasarić, Z. Diurnal Internal Tides Detected in the Adriatic. *Ann. Geophys.* **2006**, *24*, 2773–2780. [CrossRef]
22. Novosel, M.; Požar-Domac, A.; Pasarić, M. Diversity and Distribution of the Bryozoa along Underwater Cliffs in the Adriatic Sea with Special Reference to Thermal Regime. *Mar. Ecol.* **2004**, *25*, 155–170. [CrossRef]
23. Orlić, M.; Beg Paklar, G.; Dadić, V.; Leder, N.; Mihanović, H.; Pasarić, M.; Pasarić, Z. Diurnal Upwelling Resonantly Driven by Sea Breezes around an Adriatic Island. *J. Geophys. Res.* **2011**, *116*, C09025. [CrossRef]
24. Zavatarelli, M.; Raicich, F.; Bregant, D.; Russo, A.; Artegiani, A. Climatological Biogeochemical Characteristics of the Adriatic Sea. *J. Mar. Syst.* **1998**, *18*, 227–263. [CrossRef]
25. Utermöhl, H. Zur Vervollkommnung der quantitativen Phytoplankton-Methodik (Towards a perfection of quantitative phytoplankton methodology). *Mitt. Int. Ver. Theor. Angew. Limnol.* **1958**, *9*, 1–38. [CrossRef]
26. Babić, I.; Mucko, M.; Petrić, I.; Bosak, S.; Mihanović, H.; Vilibić, I.; Dupčić Radić, I.; Cetinić, I.; Balestra, C.; Casotti, R.; et al. Multilayer Approach for Characterization of Bacterial Diversity in a Marginal Sea: From Surface to Seabed. *J. Mar. Syst.* **2018**, *184*, 15–27. [CrossRef]
27. Becker, S.; Aoyama, M.; Woodward, E.; Bakker, K.; Coverly, S.; Mahaffey, C.; Tanhua, T. GO-SHIP Repeat Hydrography Nutrient Manual: The Precise and Accurate Determination of Dissolved Inorganic Nutrients in Seawater, Using Continuous Flow Analysis Methods. *Front. Mar. Sci.* **2020**, *7*, 581790. [CrossRef]
28. Holm-Hansen, O.; Lorenzen, C.J.; Holmes, R.W.; Strickland, J.D.H. Fluorometric Determination of Chlorophyll. *ICES J. Mar. Sci.* **1965**, *30*, 3–15. [CrossRef]
29. Andrews, S. Babraham Bioinformatics— FastQC A Quality Control Tool for High Throughput Sequence Data. Available online: https://www.bioinformatics.babraham.ac.uk/projects/fastqc/ (accessed on 5 December 2022).
30. Bolyen, E.; Rideout, J.R.; Dillon, M.R.; Bokulich, N.A.; Abnet, C.C.; Al-Ghalith, G.A.; Alexander, H.; Alm, E.J.; Arumugam, M.; Asnicar, F.; et al. Reproducible, Interactive, Scalable and Extensible Microbiome Data Science Using QIIME 2. *Nat. Biotechnol.* **2019**, *37*, 852–857. [CrossRef] [PubMed]
31. Callahan, B.J.; McMurdie, P.J.; Rosen, M.J.; Han, A.W.; Johnson, A.J.A.; Holmes, S.P. DADA2: High-Resolution Sample Inference from Illumina Amplicon Data. *Nat. Methods* **2016**, *13*, 581–583. [CrossRef]
32. Guillou, L.; Bachar, D.; Audic, S.; Bass, D.; Berney, C.; Bittner, L.; Boutte, C.; Burgaud, G.; de Vargas, C.; Decelle, J.; et al. The Protist Ribosomal Reference Database (PR2): A Catalog of Unicellular Eukaryote Small Sub-Unit RRNA Sequences with Curated Taxonomy. *Nucleic Acids Res.* **2013**, *41*, D597–D604. [CrossRef]
33. Letunic, I.; Bork, P. Interactive Tree Of Life (ITOL) v4: Recent Updates and New Developments. *Nucleic Acids Res.* **2019**, *47*, W256–W259. [CrossRef]
34. Bisanz, J.E. Qiime2R: Importing QIIME2 Artifacts and Associated Data into R Sessions. Available online: https://github.com/jbisanz/qiime2R (accessed on 5 December 2022).
35. McMurdie, P.J.; Holmes, S. Phyloseq: An R Package for Reproducible Interactive Analysis and Graphics of Microbiome Census Data. *PLoS ONE* **2013**, *8*, e61217. [CrossRef] [PubMed]

36. Wickham, H.; Chang, W.; Henry, L.; Pedersen, T.L.; Takahashi, K.; Wilke, C.; Woo, K.; Yutani, H.; Dunnington, D.; Rstudio. Ggplot2: Create Elegant Data Visualisations Using the Grammar of Graphics. 2022. Available online: https://CRAN.R-project.org/package=ggplot2 (accessed on 22 December 2022).
37. Oksanen, J.; Simpson, G.L.; Blanchet, F.G.; Kindt, R.; Legendre, P.; Minchin, P.R.; O'Hara, R.B.; Solymos, P.; Stevens, M.H.H.; Szoecs, E.; et al. Vegan: Community Ecology Package. 2022. Available online: https://CRAN.R-project.org/package=vegan (accessed on 22 December 2022).
38. Harrel, F.E., Jr.; Dupont, C. Hmisc: Harrell Miscellaneous. 2022. Available online: https://CRAN.R-project.org/package=Hmisc (accessed on 22 December 2022).
39. Wickham, H.; Rstudio. Tidyverse: Easily Install. and Load. The "Tidyverse". 2022. Available online: https://CRAN.R-project.org/package=tidyverse (accessed on 22 December 2022).
40. Müller, K.; Wickham, H.; Francois, R.; Bryan, J.; Rstudio. Tibble: Simple Data Frames. 2022. Available online: https://CRAN.R-project.org/package=tibble (accessed on 22 December 2022).
41. Wickham, H.; Hester, J.; Francois, R.; Bryan, J.; Bearrows, S.; RStudio. Readr: Read Rectangular Text Data. 2022. Available online: https://github.com/mandreyel/ (accessed on 22 December 2022).
42. Viličić, D.; Vučak, Z.; Škrivanić, A.; Gržetić, Z. Phytoplankton Blooms in the Oligotrophic Open South Adriatic Waters. *Mar. Chem.* **1989**, *28*, 89–107. [CrossRef]
43. Viličić, D. Phytoplankton Taxonomy and Distribution in the Offshore Southern Adriatic. *Nat. Croat.* **1998**, *7*, 127–141.
44. Viličić, D.; Terzić, S.; Ahel, M.; Burić, Z.; Jasprica, N.; Carić, M.; Caput Mihalić, K.; Olujić, G. Phytoplankton Abundance and Pigment Biomarkers in the Oligotrophic, Eastern Adriatic Estuary. *Environ. Monit. Assess.* **2008**, *142*, 199–218. [CrossRef] [PubMed]
45. Jasprica, N.; Caric, M.; Kršinić, F.; Kapetanović, T.; Batistić, M.; Njire, J. Planktonic Diatoms and Their Environment in the Lower Neretva River Estuary (Eastern Adriatic Sea, NE Mediterranean). *Nova Hedwig.* **2012**, *141*, 405–430.
46. Viličić, D.; Jasprica, N.; Carić, M.; Burić, Z. Taxonomic Composition and Seasonal Distribution of Microphytoplankton in Mali Ston Bay (Eastern Adriatic). *Acta Bot. Croat.* **1998**, *57*, 29–48.
47. Drakulović, D.; Krivokapić, S.; Mandić, M.; Redžic, A. Phytoplankton Community in Boka Kotorska Bay (South-Eastern Adriatic). *Rapp. Comm. Int. Mer. Médit.* **2013**, *40*, 428.
48. La Ferla, R.; Maimone, G.; Azzaro, M.; Conversano, F.; Brunet, C.; Cabral, A.S.; Paranhos, R. Vertical Distribution of the Prokaryotic Cell Size in the Mediterranean Sea. *Helgol. Mar. Res.* **2012**, *66*, 635–650. [CrossRef]
49. Viličić, D.; Marasović, I.; Mioković, D. Checklist of Phytoplankton in the Eastern Adriatic Sea. *Acta Bot. Croat.* **2002**, *61*, 57–91.
50. Viličić, D.; Leder, N.; Gržetić, Z.; Jasprica, N. Microphytoplankton in the Strait of Otranto (Eastern Mediterranean). *Mar. Biol.* **1995**, *123*, 619–630. [CrossRef]
51. Turchetto, M.; Bianchi, F.; Boldrin, A.; Malaguti, A.; Rabitti, S.; Socal, G.; Strada, L. Nutrients, Phytoplankton and Primary Production Processes in Oligotrophic Areas (Southern Adriatic and Northern Ionian). *Atti AIOL* **2000**, *13*, 269–278.
52. Socal, G.; Boldrin, A.; Bianchi, F.; Civitarese, G.; De Lazzari, A.; Rabitti, S.; Totti, C.; Turchetto, M.M. Nutrient, Particulate Matter and Phytoplankton Variability in the Photic Layer of the Otranto Strait. *J. Mar. Syst.* **1999**, *20*, 381–398. [CrossRef]
53. Čalić, M.; Carić, M.; Kršinić, F.; Jasprica, N.; Pećarević, M. Controlling Factors of Phytoplankton Seasonal Succession in Oligotrophic Mali Ston Bay (South-Eastern Adriatic). *Environ. Monit. Assess.* **2013**, *185*, 7543–7563. [CrossRef] [PubMed]
54. Krivokapić, S.; Bosak, S.; Viličić, D.; Kušpilić, G.; Drakulović, D.; Pestorić, B. Algal Pigments Distribution and Phytoplankton Group Assemblages in Coastal Transitional Environment—Boka Kotorska Bay (South Eastern Adriatic Sea). *Acta Adriat.* **2018**, *59*, 35–49. [CrossRef]
55. Viličić, D. A Study of Phytoplankton in the Adriatic Sea after the July 1984 Bloom. *Int. Rev. Ges. Hydrobiol.* **1991**, *76*, 197–211. [CrossRef]
56. Decembrini, F.; Caroppo, C.; Azzaro, M. Size Structure and Production of Phytoplankton Community and Carbon Pathways Channelling in the Southern Tyrrhenian Sea (Western Mediterranean). *Deep. Sea Res. Part. II Top. Stud. Oceanogr.* **2009**, *56*, 687–699. [CrossRef]
57. Turley, C.M. The Changing Mediterranean Sea—A Sensitive Ecosystem? *Prog. Oceanogr.* **1999**, *44*, 387–400. [CrossRef]
58. Yahia-Kefi, D.O.; Souissi, S.; Gomez, F.; Daly Yahia, M.N. Spatio-Temporal Distribution of the Dominant Diatom and Dinoflagellate Species in the Bay of Tunis (SW Mediterranean Sea). *Medit. Mar. Sci.* **2005**, *6*, 17. [CrossRef]
59. Becacos-Kontos, T. Primary Production and Environmental Factors in an Oligotrophic Biome in the Aegean Sea. *Mar. Biol.* **1977**, *42*, 93–98. [CrossRef]
60. Berman, T.; Townsend, D.; Elsayed, S.; Trees, C.; Azov, Y. Optical Transparency, Chlorophyll and Primary Productivity in the Eastern Mediterranean near the Israeli Coast. *Oceanol. Acta* **1984**, *7*, 367–372.
61. Thingstad, T.F.; Sakshaug, E. Control of Phytoplankton Growth in Nutrient Recycling Ecosystems. Theory and Terminology. *Mar. Ecol. Prog. Ser.* **1990**, *63*, 261–272. [CrossRef]
62. Estrada, M.; Blasco, D. Two Phases of the Phytoplankton Community in the Baja California Upwelling1. *Limnol. Oceanogr.* **1979**, *24*, 1065–1080. [CrossRef]
63. Viličić, D. Phytoplankton Communities of the South Adriatic in the Greater Vicinity of Dubrovnik. *Acta Bot. Croat.* **1984**, *43*, 175–189.

64. Pestorić, B.; Drakulović, D.; Mandić, M.; López Abbate, C. Distribution Changes of Plankton Communities in the Harbour Porto Montenegro (South Adriatic Sea). *Stud. Mar.* **2018**, *31*, 5–31. [CrossRef]
65. Siokou-Frangou, I.; Christaki, U.; Mazzocchi, M.G.; Montresor, M.; Ribera d'Alcalá, M.; Vaqué, D.; Zingone, A. Plankton in the Open Mediterranean Sea: A Review. *Biogeosciences* **2010**, *7*, 1543–1586. [CrossRef]
66. Ignatiades, L.; Gotsis-Skretas, O.; Pagou, K.; Krasakopoulou, E. Diversification of Phytoplankton Community Structure and Related Parameters along a Large-Scale Longitudinal East-West Transect of the Mediterranean Sea. *J. Plankton Res.* **2009**, *31*, 411–428. [CrossRef]
67. Ninčević Gladan, Ž.; Matić, F.; Arapov, J.; Skejić, S.; Bužančić, M.; Bakrač, A.; Straka, M.; Dekneudt, Q.; Grbec, B.; Garber, R.; et al. The Relationship between Toxic Phytoplankton Species Occurrence and Environmental and Meteorological Factors along the Eastern Adriatic Coast. *Harmful Algae* **2020**, *92*, 101745. [CrossRef] [PubMed]
68. Massana, R.; Pernice, M.; Bunge, J.A.; Campo, J. del Sequence Diversity and Novelty of Natural Assemblages of Picoeukaryotes from the Indian Ocean. *ISME J.* **2011**, *5*, 184–195. [CrossRef]
69. Clarke, L.J.; Bestley, S.; Bissett, A.; Deagle, B.E. A Globally Distributed Syndiniales Parasite Dominates the Southern Ocean Micro-Eukaryote Community near the Sea-Ice Edge. *ISME J.* **2019**, *13*, 734–737. [CrossRef] [PubMed]
70. Piredda, R.; Tomasino, M.P.; D'Erchia, A.M.; Manzari, C.; Pesole, G.; Montresor, M.; Kooistra, W.H.C.F.; Sarno, D.; Zingone, A. Diversity and Temporal Patterns of Planktonic Protist Assemblages at a Mediterranean Long Term Ecological Research Site. *FEMS Microbiol. Ecol.* **2017**, *93*, fiw200. [CrossRef]
71. Mucko, M.; Bosak, S.; Casotti, R.; Balestra, C.; Ljubešić, Z. Winter Picoplankton Diversity in an Oligotrophic Marginal Sea. *Mar. Genom.* **2018**, *42*, 14–24. [CrossRef]
72. Rowena, S.; Picard, K.; Clarke, J.; Walker, C.; Martins, C.; Marshall, C.; Amorim, A.; Woodward, M.; Widdicombe, C.; Tarran, G.; et al. Composition and Patterns of Taxa Assemblages in the Western Channel Assessed by 18S Sequencing, Microscopy and Flow Cytometry. *J. Mar. Sci. Eng.* **2023**, *11*, 480.
73. Piredda, R.; Claverie, J.-M.; Decelle, J.; de Vargas, C.; Dunthorn, M.; Edvardsen, B.; Eikrem, W.; Forster, D.; Kooistra, W.H.C.F.; Logares, R.; et al. Diatom Diversity through HTS-Metabarcoding in Coastal European Seas. *Sci. Rep.* **2018**, *8*, 18059. [CrossRef]
74. Ujević, I.; Ninčević-Gladan, Z.; Roje, R.; Skejić, S.; Arapov, J.; Marasović, I. Domoic Acid—A New Toxin in the Croatian Adriatic Shellfish Toxin Profile. *Molecules* **2010**, *15*, 6835–6849. [CrossRef] [PubMed]
75. Mochemadkar, S.; Gauns, M.; Pratihary, A.; Thorat, B.; Roy, R.; Pai, I.K.; Naqvi, S. Response of Phytoplankton to Nutrient Enrichment with High Growth Rates in a Tropical Monsoonal Estuary—Zuari Estuary, India. *Indian. J. Geo-Mar. Sci.* **2013**, *42*, 314–325.
76. Revelante, N.; Gilmartin, M. Microplankton Diversity Indices as Indicators of Eutrophication in the Northern Adriatic Sea. *Hydrobiologia* **1980**, *70*, 277–286. [CrossRef]
77. Pucher-Petković, T.; Marasović, I. Développement Des Populations Phytoplanctoniques Caractéristiques Pour Un Milieu Eutrophisé (Baie de Kaštela, Adriatique Centrale). *Acta Adriat.* **1980**, *21*, 79–93.
78. Boldrin, A.; Miserocchi, S.; Rabitti, S.; Turchetto, M.M.; Balboni, V.; Socal, G. Particulate Matter in the Southern Adriatic and Ionian Sea: Characterisation and Downward Fluxes. *J. Mar. Syst.* **2002**, *33–34*, 389–410. [CrossRef]
79. Berland, B.; Burlakova, Z.P.; Georgieva, L.; Izmestieva, M.; Kholodov, V.; Krupatkina, D.K.; Maestrini, S.; Zaika, V.E. Phytoplancton Estival de La Mer Du Levant, Biomasse et Facteurs Limitants. *Prod. Relat. Trophique Ecosystèmes Mar.* **1987**, *2*, 61–83.
80. Gotsis-Skretas, O.; Pagou, K.; Moraitou-Apostolopoulou, M.; Ignatiades, L. Seasonal Horizontal and Vertical Variability in Primary Production and Standing Stocks of Phytoplankton and Zooplankton in the Cretan Sea and the Straits of the Cretan Arc (March 1994–January 1995). *Prog. Oceanogr.* **1999**, *44*, 625–649. [CrossRef]
81. Latasa, M.; Estrada, M.; Delgado, M. Plankton-Pigment Relationships in the Northwestern Mediterranean during Stratification. *Mar. Ecol. Prog. Ser.* **1992**, *88*, 61–73. [CrossRef]
82. Kimor, B. Distinctive Features of the Plankton of the Eastern Mediterranean. *Annls. Inst. Oceanogr.* **1983**, *59*, 97–106.
83. Kimor, B.; Berman, T.; Schneller, A. Phytoplankton Assemblages in the Deep Chlorophyll Maximum Layers off the Mediterranean Coast of Israel. *J. Plankton Res.* **1987**, *9*, 433–443. [CrossRef]
84. Drakulović, D.; Vuksanović, N.; Joksimović, D. Dynamics of Phytoplankton in Boka Kotorska Bay. *Stud. Mar.* **2010**, *25*, 1–20.
85. Burić, Z.; Cetinić, I.; Viličić, D.; Mihalić, K.C.; Carić, M.; Olujić, G. Spatial and Temporal Distribution of Phytoplankton in a Highly Stratified Estuary (Zrmanja, Adriatic Sea). *Mar. Ecol.* **2007**, *28*, 169–177. [CrossRef]
86. Vidussi, F.; Claustre, H.; Manca, B.B.; Luchetta, A.; Marty, J.-C. Phytoplankton Pigment Distribution in Relation to Upper Thermocline Circulation in the Eastern Mediterranean Sea during Winter. *J. Geophys. Res. Ocean.* **2001**, *106*, 19939–19956. [CrossRef]
87. Marty, J.-C.; Chiavérini, J. Seasonal and Interannual Variations in Phytoplankton Production at DYFAMED Time-Series Station, Northwestern Mediterranean Sea. *Deep. Sea Res. Part. II Top. Stud. Oceanogr.* **2002**, *49*, 2017–2030. [CrossRef]
88. Viličić, D. A Phytoplankton Study of Southern Adriatic Waters near Dubrovnik for the Period from June 1979 to July 1980. *CENTRO* **1985**, *1*, 35–36.
89. Estrada, M. Phytoplankton Assemblages across a NW Mediterranean Front: Changes from Winter Mixing to Spring Stratification. *Oecol. Aquatic.* **1991**, *10*, 157–185.
90. Giaccone, G.; Geraci, R. Biogeografia Delle Alghe Del Mediterráneo. *An. Jard. Bot. Madr.* **1989**, *1*, 27–34.

91. Gómez, F. Endemic and Indo-Pacific Plankton in the Mediterranean Sea: A Study Based on Dinoflagellate Records. *J. Biogeogr.* **2006**, *33*, 261–270. [CrossRef]
92. Skejić, S.; Arapov, J.; Kovačević, V.; Bužančić, M.; Bensi, M.; Giani, M.; Bakrač, A.; Mihanović, H.; Gladan, Ž.N.; Urbini, L.; et al. Coccolithophore Diversity in Open Waters of the Middle Adriatic Sea in Pre- and Post-Winter Periods. *Mar. Micropaleontol.* **2018**, *143*, 30–45. [CrossRef]
93. Cros, L.; Fortuño, J.M. Atlas of Northwestern Mediterranean Coccolithophores. *Sci. Mar.* **2002**, *66*, 1–182. [CrossRef]
94. Estrada, M.; Marrase, C.; Latasa, M.; Berdalet, E.; Delgado, M.; Riera, T. Variability of Deep Chlorophyll Maximum Characteristics in the Northwestern Mediterranean. *Mar. Ecol. Prog. Ser.* **1993**, *92*, 289–300. [CrossRef]
95. Gran-Stadniczeñko, S.; Egge, E.; Hostyeva, V.; Logares, R.; Eikrem, W.; Edvardsen, B. Protist Diversity and Seasonal Dynamics in Skagerrak Plankton Communities as Revealed by Metabarcoding and Microscopy. *J. Eukaryot. Microbiol.* **2019**, *66*, 494–513. [CrossRef] [PubMed]
96. Lohrenz, S.E.; Arnone, R.A.; Wiesenburg, D.A.; DePalma, I.P. Satellite Detection of Transient Enhanced Primary Production in the Western Mediterranean Sea. *Nature* **1988**, *335*, 245–247. [CrossRef]
97. Magazzù, G.; Decembrini, F. Primary Production, Biomass and Abundance of Phototrophic Picoplankton in the Mediterranean Sea: A Review. *Aquat. Microb. Ecol.* **1995**, *9*, 97–104. [CrossRef]
98. Wang, F.; Huang, B.; Xie, Y.; Cai, S.; Wang, X.; Mu, J. Diversity, Composition, and Activities of Nano- and Pico-Eukaryotes in the Northern South China Sea With Influences of Kuroshio Intrusion. *Front. Mar. Sci.* **2021**, *8*, 658233. [CrossRef]
99. Mena, C.; Reglero, P.; Hidalgo, M.; Sintes, E.; Santiago, R.; Martín, M.; Moyà, G.; Balbín, R. Phytoplankton Community Structure Is Driven by Stratification in the Oligotrophic Mediterranean Sea. *Front. Microbiol.* **2019**, *10*, 1698. [CrossRef]
100. De Vargas, C.; Audic, S.; Henry, N.; Decelle, J.; Mahé, F.; Logares, R.; Lara, E.; Berney, Ć.; Le Bescot, N.; Probert, I.; et al. Eukaryotic Plankton Diversity in the Sunlit Ocean. *Science* **2015**, *348*, 1261605. [CrossRef]
101. Margalef, R. Composición Específica Del Fitoplancton de La Costa Catalano-Levantina (Mediterráneo Occidental) En 1962–1967. *Geography* **1969**, *33*, 345–380.
102. Šantić, D.; Piwosz, K.; Matić, F.; Vrdoljak Tomaš, A.; Arapov, J.; Dean, J.L.; Šolić, M.; Koblížek, M.; Kušpilić, G.; Šestanović, S. Artificial Neural Network Analysis of Microbial Diversity in the Central and Southern Adriatic Sea. *Sci. Rep.* **2021**, *11*, 11186. [CrossRef]
103. Šantić, D.; Vrdoljak Tomaš, A.; Lušić, J. Spatial and Temporal Patterns of Picoplankton Community in the Central and Southern Adriatic Sea. In *The Montenegrin Adriatic Coast: Marine Biology*; Joksimović, A., Đurović, M., Zonn, I.S., Kostianoy, A.G., Semenov, A.V., Eds.; The Handbook of Environmental Chemistry; Springer International Publishing: Cham, Switzerland, 2020; pp. 29–51. ISBN 978-3-030-77513-1.
104. Mackey, K.R.M.; Paytan, A.; Caldeira, K.; Grossman, A.R.; Moran, D.; McIlvin, M.; Saito, M.A. Effect of Temperature on Photosynthesis and Growth in Marine *Synechococcus* Spp. *Plant. Physiol.* **2013**, *163*, 815–829. [CrossRef] [PubMed]
105. Hafner, D.; Car, A.; Jasprica, N.; Kapetanović, T.; Radić, I.D. Relationship between Marine Epilithic Diatoms and Environmental Variables in Oligotrophic Bay, NE Mediterranean. *Mediterr. Mar. Sci.* **2018**, *19*, 223–239. [CrossRef]
106. Civitarese, G.; Crise, A.; Crispi, G.; Mosetti, R. Circulation Effects on Nitrogen Dynamics in the Ionian Sea. *Oceanol. Acta* **1996**, *19*, 609–622.
107. Dolan, J.R.; Vidussi, F.; Claustre, H. Planktonic Ciliates in the Mediterranean Sea: Longitudinal Trends. *Deep. Sea Res. Part I Oceanogr. Res. Pap.* **1999**, *46*, 2025–2039. [CrossRef]
108. Šantić, D.; Krstulović, N.; Šolić, M.; Ordulj, M.; Kušpilić, G. Dynamics of Prokaryotic Picoplankton Community in the Central and Southern Adriatic Sea (Croatia). *Helgol. Mar. Res.* **2013**, *67*, 471–481. [CrossRef]
109. Larkin, A.A.; Blinebry, S.K.; Howes, C.; Lin, Y.; Loftus, S.E.; Schmaus, C.A.; Zinser, E.R.; Johnson, Z.I. Niche Partitioning and Biogeography of High Light Adapted Prochlorococcus across Taxonomic Ranks in the North Pacific. *ISME J.* **2016**, *10*, 1555–1567. [CrossRef]
110. Mella-Flores, D.; Mazard, S.; Humily, F.; Partensky, F.; Mahé, F.; Bariat, L.; Courties, C.; Marie, D.; Ras, J.; Mauriac, R.; et al. Is the Distribution of *Prochlorococcus* and *Synechococcus* Ecotypes in the Mediterranean Sea Affected by Global Warming? *Biogeosciences* **2011**, *8*, 2785–2804. [CrossRef]
111. Zwirglmaier, K.; Jardillier, L.; Ostrowski, M.; Mazard, S.; Garczarek, L.; Vaulot, D.; Not, F.; Massana, R.; Ulloa, O.; Scanlan, D.J. Global Phylogeography of Marine Synechococcus and Prochlorococcus Reveals a Distinct Partitioning of Lineages among Oceanic Biomes. *Env. Microbiol.* **2008**, *10*, 147–161. [CrossRef]
112. Coello-Camba, A.; Agustí, S. Picophytoplankton Niche Partitioning in the Warmest Oligotrophic Sea. *Front. Mar. Sci.* **2021**, *8*, 651877. [CrossRef]
113. Schmoker, C.; Hernández-León, S. Stratification Effects on the Plankton of the Subtropical Canary Current. *Prog. Oceanogr.* **2013**, *119*, 24–31. [CrossRef]
114. Šilović, T.; Mihanović, H.; Batistić, M.; Radić, I.D.; Hrustić, E.; Najdek, M. Picoplankton Distribution Influenced by Thermohaline Circulation in the Southern Adriatic. *Cont. Shelf Res.* **2018**, *155*, 21–33. [CrossRef]
115. Moore, L.R.; Post, A.F.; Rocap, G.; Chisholm, S.W. Utilization of Different Nitrogen Sources by the Marine Cyanobacteria Prochlorococcus and Synechococcus. *Limnol. Oceanogr.* **2002**, *47*, 989–996. [CrossRef]

116. Duarte, C.M.; Agustí, S.; Gasol, J.M.; Vaqué, D.; Vazquez-Dominguez, E. Effect of Nutrient Supply on the Biomass Structure of Planktonic Communities: An Experimental Test on a Mediterranean Coastal Community. *Mar. Ecol. Prog. Ser.* **2000**, *206*, 87–95. [CrossRef]
117. Jardillier, L.; Boucher, D.; Personnic, S.; Jacquet, S.; Thénot, A.; Sargos, D.; Amblard, C.; Debroas, D. Relative Importance of Nutrients and Mortality Factors on Prokaryotic Community Composition in Two Lakes of Different Trophic Status: Microcosm Experiments. *FEMS Microbiol. Ecol.* **2005**, *53*, 429–443. [CrossRef] [PubMed]
118. Pittera, J.; Humily, F.; Thorel, M.; Grulois, D.; Garczarek, L.; Six, C. Connecting Thermal Physiology and Latitudinal Niche Partitioning in Marine Synechococcus. *ISME J.* **2014**, *8*, 1221–1236. [CrossRef]
119. Korlević, M.; Pop RIstova, P.; Garić, R.; Amann, R.; Orlić, S. Bacterial Diversity in the South Adriatic Sea during a Strong Deep Winter Convection Year. *Appl. Environ. Microbiol.* **2015**, *81*, 1715–1726. [CrossRef] [PubMed]
120. Šantić, D.; Kovačević, V.; Bensi, M.; Giani, M.; Vrdoljak Tomaš, A.; Ordulj, M.; Santinelli, C.; Šestanović, S.; Šolić, M.; Grbec, B. Picoplankton Distribution and Activity in the Deep Waters of the Southern Adriatic Sea. *Water* **2019**, *11*, 1655. [CrossRef]
121. Henley, W.J.; Hironaka, J.L.; Guillou, L.; Buchheim, M.A.; Buchheim, J.A.; Fawley, M.W.; Fawley, K.P. Phylogenetic Analysis of the 'Nannochloris-like' Algae and Diagnoses of Picochlorum Oklahomensis Gen. et Sp. Nov. (Trebouxiophyceae, Chlorophyta). *Phycologia* **2004**, *43*, 641–652. [CrossRef]
122. Claustre, H.; Sciandra, A.; Vaulot, D. Introduction to the Special Section Bio-Optical and Biogeochemical Conditions in the South East Pacific in Late 2004: The BIOSOPE Program. *Biogeosciences* **2008**, *5*, 679–691. [CrossRef]
123. Shi, X.L.; Marie, D.; Jardillier, L.; Scanlan, D.J.; Vaulot, D. Groups without Cultured Representatives Dominate Eukaryotic Picophytoplankton in the Oligotrophic South East Pacific Ocean. *PLoS ONE* **2009**, *4*, e7657. [CrossRef]
124. Sherr, E.B.; Sherr, B.F. Bacterivory and Herbivory: Key Roles of Phagotrophic Protists in Pelagic Food Webs. *Microb. Ecol.* **1994**, *28*, 223–235. [CrossRef] [PubMed]
125. Turk, V.; Lučić, D.; Njire, J.; Terzić, S.; Tinta, T.; Benović, A.; Malej, A. The Epiplankton Community in the Southern Adriatic: Multiple Trophic Levels along the South–North and Inshore–Offshore Gradients. *Acta Adriatica* **2012**, *53*, 263–276.
126. Gallina, A.A.; Celussi, M.; Del Negro, P. Large-Scale Distribution and Production of Bacterioplankton in the Adriatic Sea. *J. Sea Res.* **2011**, *66*, 1–8. [CrossRef]
127. Yeh, Y.-C.; Fuhrman, J.A. Contrasting Diversity Patterns of Prokaryotes and Protists over Time and Depth at the San-Pedro Ocean Time Series. *ISME Commun.* **2022**, *2*, 36. [CrossRef]
128. Campbell, L.; Gaonkar, C.C.; Henrichs, D.W. Chapter 5—Integrating Imaging and Molecular Approaches to Assess Phytoplankton Diversity. In *Advances in Phytoplankton Ecology*; Clementson, L.A., Eriksen, R.S., Willis, A., Eds.; Elsevier: Amsterdam, The Netherlands, 2022; pp. 159–190. ISBN 978-0-12-822861-6.